

Observation of the $\Xi_b^- \rightarrow \psi(2S)\Xi^-$ decay and studies of the $\Xi_b(5945)^0$ baryon in proton-proton collisions at $\sqrt{s} = 13$ TeV

A. Hayrapetyan *et al.*^{*}
(CMS Collaboration)



(Received 27 February 2024; accepted 15 May 2024; published 8 July 2024)

The first observation of the decay $\Xi_b^- \rightarrow \psi(2S)\Xi^-$ and measurement of the branching ratio of $\Xi_b^- \rightarrow \psi(2S)\Xi^-$ to $\Xi_b^- \rightarrow J/\psi\Xi^-$ are presented. The J/ψ and $\psi(2S)$ mesons are reconstructed using their dimuon decay modes. The results are based on proton-proton colliding beam data from the LHC collected by the CMS experiment at $\sqrt{s} = 13$ TeV in 2016–2018, corresponding to an integrated luminosity of 140 fb^{-1} . The branching fraction ratio is measured to be $\mathcal{B}(\Xi_b^- \rightarrow \psi(2S)\Xi^-)/\mathcal{B}(\Xi_b^- \rightarrow J/\psi\Xi^-) = 0.84^{+0.21}_{-0.19}(\text{stat}) \pm 0.10(\text{syst}) \pm 0.02(\mathcal{B})$, where the last uncertainty comes from the uncertainties in the branching fractions of the charmonium states. New measurements of the $\Xi_b(5945)^0$ baryon mass and natural width are also presented, using the $\Xi_b^-\pi^+$ final state, where the Ξ_b^- baryon is reconstructed through the decays $J/\psi\Xi^-$, $\psi(2S)\Xi^-$, $J/\psi\Lambda K^-$, and $J/\psi\Sigma^0 K^-$. Finally, the fraction of Ξ_b^- baryons produced from $\Xi_b(5945)^0$ decays is determined.

DOI: 10.1103/PhysRevD.110.012002

I. INTRODUCTION

The Ξ_b family consists of baryons that form isodoublets composed of a triplet of b , s , and q quarks, where q corresponds to a u or d quark for the Ξ_b^0 and Ξ_b^- states, respectively. Three such isodoublets that are neither orbitally nor radially excited should exist [1]. These include one with the spin of the light diquark $j_{qs} = 0$ and spin-parity of the baryon $J^P = 1/2^+$ (Ξ_b ground states), one with $j_{qs} = 1$ and $J^P = 1/2^+$ (Ξ'_b), and another with $j_{qs} = 1$ and $J^P = 3/2^+$ (Ξ^*_b). The ground states were discovered more than a decade ago at the Fermilab Tevatron [2–4] via their decays to $J/\psi\Xi^-$ and $\Xi_c^+\pi^-$. Three of the four states with $j_{qs} = 1$ have been observed during the last decade at the CERN LHC [5–7] via their $\Xi_b^-\pi^+$ and $\Xi_b^0\pi^-$ decays, as expected from theoretical predictions [8–10]. The fourth state, Ξ_b^0 , is expected to have a mass lower than the $\Xi_b^-\pi^+$ mass threshold, making a strong decay to the Ξ_b^- baryon kinematically impossible. Several other more massive Ξ_b resonances were also observed recently by the CMS and LHCb Collaborations [11–15] via their decays to $\Xi_b^0\pi^-$, $\Xi_b^-\pi^+$, $\Xi_b^-\pi^+\pi^-$, $\Xi_b^0\pi^+\pi^-$, $\Lambda_b^0K^-$, and $\Lambda_b^0K^-\pi^+$. Various theoretical models and calculations predict a spectrum of

excited Ξ_b baryons [8–10,16–27], and the observed resonances are considered to be $1P$ isodoublets of Ξ_b or Ξ'_b states, and a $1D$ doublet. However, larger data samples are needed to measure the quantum numbers of these resonances. There is also the possibility that some of the observed wide resonances could instead be unresolved overlapping narrow states.

Besides the searches for excited Ξ_b states, the LHCb Collaboration has observed new ground-state Ξ_b decays and determined some of their branching fractions [28–33]. The spectrum of excited Ξ_b baryons can be classified relatively easily, especially with the guidance of the similar and well-established Ξ_c baryons [34]. By contrast, the wide variety of decay modes available in the weak decay of the ground-state baryons presents a significant theoretical challenge, and predictions of the branching fractions to various final states are less straightforward. Multibody decays of Ξ_b baryons can contain rich resonant structures, including both conventional and exotic resonances, such as excited Ξ^- states and the $P_{\psi s}^\Lambda(4459)^0$ pentaquark reported in the $\Xi_b^- \rightarrow J/\psi\Lambda K^-$ decay [35]. The search for new Ξ_b decays is also important in the quest for observing possible CP violation [36]. In general, both weak decays of heavy baryons and their strongly decaying excitations can be described in the framework of heavy-quark effective theory (HQET) [37–41]. Measurements of the decays and properties of both ground and excited Ξ_b states provide coherent and complementary input to HQET, which could improve our understanding of the quantum chromodynamic (QCD) mechanisms responsible for quark dynamics and the formation of hadrons.

*Full author list given at the end of the article.

In this paper, we study Ξ_b^- and $\Xi_b(5945)^0$ (also referred to as Ξ_b^{*0} here) baryon states using a sample of proton-proton (pp) collisions from the LHC, collected by the CMS experiment in 2016–2018 at $\sqrt{s} = 13$ TeV, corresponding to an integrated luminosity of 140 fb^{-1} [42–44]. The inclusion of charge-conjugate states is implied throughout this paper, unless otherwise noted. We report the first observation of the $\Xi_b^- \rightarrow \psi(2S)\Xi^-$ decay and the measurement of its branching fraction with respect to the well-known $\Xi_b^- \rightarrow J/\psi\Xi^-$ decay. In both signal and normalization channels, the charmonium states are reconstructed through their dimuon decay modes, and Ξ^- decays to $\Lambda\pi^-$ with the following $\Lambda \rightarrow p\pi^-$ are used. Thus, the relative branching ratio R is measured using the following expression:

$$R = \frac{\mathcal{B}(\Xi_b^- \rightarrow \psi(2S)\Xi^-)}{\mathcal{B}(\Xi_b^- \rightarrow J/\psi\Xi^-)} = \frac{N(\Xi_b^- \rightarrow \psi(2S)\Xi^-)}{N(\Xi_b^- \rightarrow J/\psi\Xi^-)} \times \frac{\epsilon(\Xi_b^- \rightarrow J/\psi\Xi^-)}{\epsilon(\Xi_b^- \rightarrow \psi(2S)\Xi^-)} \frac{\mathcal{B}(J/\psi \rightarrow \mu^+\mu^-)}{\mathcal{B}(\psi(2S) \rightarrow \mu^+\mu^-)}, \quad (1)$$

where N and ϵ represent the measured number of signal events in data and the total efficiency from Monte Carlo (MC) simulation, respectively, for each of the respective decay modes. The values of the branching fractions \mathcal{B} in the last term are taken from the PDG [34]. Even though the value of $\mathcal{B}(\Xi_b^- \rightarrow J/\psi\Xi^-)$ is not known, the choice of this normalization channel is quite natural since it has the same topology and similar kinematic properties as the signal channel, reducing the systematic uncertainty in the ratio related to the reconstruction of the muons and the other charged particle tracks from the Ξ_b^- decays.

We also determine the $\Xi_b(5945)^0$ baryon mass and natural width, using the $\Xi_b(5945)^0 \rightarrow \Xi_b^-\pi^+$ decay. The ground-state Ξ_b^- is reconstructed via its decays to $J/\psi\Xi^-$, $\psi(2S)\Xi^-$, and $J/\psi\Lambda K^-$. For the $\Xi_b^- \rightarrow \psi(2S)\Xi^-$ decay, both $\psi(2S) \rightarrow J/\psi\pi^+\pi^-$, with $J/\psi \rightarrow \mu^+\mu^-$, and $\psi(2S) \rightarrow \mu^+\mu^-$ modes are used in the analysis, and Ξ^- is again reconstructed via the $\Lambda\pi^-$ channel. For the $\Xi_b^- \rightarrow J/\psi\Lambda K^-$ decay, the presence of the partially reconstructed mode $J/\psi\Sigma^0K^-$, where the low-energy photon from the $\Sigma^0 \rightarrow \Lambda\gamma$ decay is undetected, is included in the fit to the $\Xi_b^-\pi^+$ invariant mass spectrum. Pictorial representations of the decay topologies for $\Xi_b(5945)^0 \rightarrow \Xi_b^-\pi^+$ are shown in Fig. 1.

We also measure the ratio of the production cross sections $R_{\Xi_b(5945)^0}$ for $\Xi_b(5945)^0$ and Ξ_b^- using the expression:

$$R_{\Xi_b(5945)^0} = \frac{\sigma(pp \rightarrow \Xi_b(5945)^0 X) \mathcal{B}(\Xi_b(5945)^0 \rightarrow \Xi_b^-\pi^+)}{\sigma(pp \rightarrow \Xi_b^- X)} = \frac{N(\Xi_b(5945)^0 \rightarrow \Xi_b^-\pi^+)}{N(\Xi_b^-)} \frac{\epsilon(\Xi_b^-)}{\epsilon(\Xi_b(5945)^0 \rightarrow \Xi_b^-\pi^+)}, \quad (2)$$

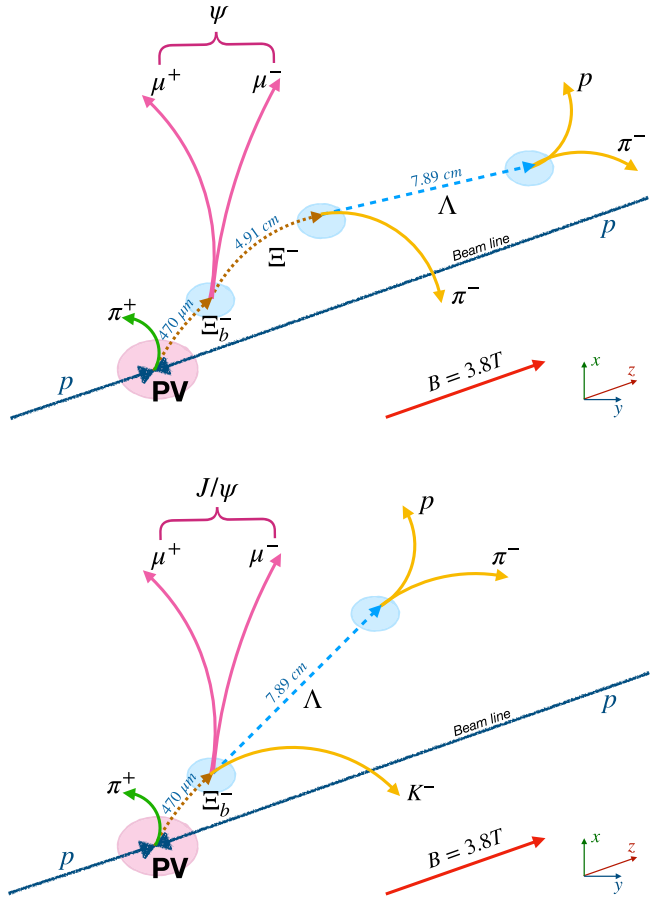


FIG. 1. The $\Xi_b(5945)^0 \rightarrow \Xi_b^-\pi^+$ decay topology in which the Ξ_b^- baryon decays to $\psi\Xi^-$ with $\psi \rightarrow \mu^+\mu^-$ (upper) or $J/\psi\Lambda K^-$ (lower), where ψ refers to the J/ψ and $\psi(2S)$ mesons. The distances given are the average decay lengths, $c\tau$.

where N and ϵ refer to similar quantities as those in Eq. (1). Following an analogous CMS measurement of the $B_c(2S)^+$ and $B_c^*(2S)^+$ production cross section ratios [45], the Ξ_b^- baryon is reconstructed in the phase space region defined by the Ξ_b^- baryon transverse momentum $p_T > 15 \text{ GeV}$ and rapidity $|y| < 2.4$; however, this measured ratio is intended to be representative of the entire phase space, given the small mass difference between the $\Xi_b(5945)^0$ and Ξ_b^- particles. The $\Xi_b(5945)^0$ baryon was the first new particle observed by the CMS Collaboration, using 5 fb^{-1} of data from 2011 [5]. With this paper we significantly improve and enrich our previous results for this state. Tabulated results are provided in the HEPData record for this analysis [46].

II. THE CMS DETECTOR AND SIMULATED EVENT SAMPLES

The central feature of the CMS apparatus is a superconducting solenoid of 6 m internal diameter, providing a magnetic field of 3.8 T. Within the solenoid volume are a silicon pixel and strip tracker, a lead tungstate crystal

electromagnetic calorimeter, and a brass and scintillator hadron calorimeter, each composed of a barrel and two end cap sections. Forward calorimeters extend the pseudorapidity (η) coverage provided by the barrel and end cap detectors. Muons are measured in gas-ionization detectors embedded in the steel flux-return yoke outside the solenoid. A more detailed description of the CMS detector, together with a definition of the coordinate system used and the relevant kinematic variables, can be found in Ref. [47]. More recent changes to the detector are described in Ref. [48].

Muons are measured in the range $|\eta| < 2.4$, with detection planes made using three technologies: drift tubes, cathode strip chambers, and resistive plate chambers. The single-muon trigger efficiency exceeds 90% over the full η range, whereas the efficiency to reconstruct and identify muons is greater than 96%. Matching muons identified in the muon system to tracks measured in the silicon tracker results in a relative p_T resolution for muons with p_T up to 100 GeV of 1% in the barrel and 3% in the end caps [49]. The silicon tracker used in 2016 measured charged particles within the range $|\eta| < 2.5$. For nonisolated particles of $1 < p_T < 10$ GeV and $|\eta| < 1.4$, the track resolutions were typically 1.5% in p_T and 25–90 (45–150) μm in the transverse (longitudinal) impact parameter [50]. At the start of 2017, a new pixel detector was installed [51]; the upgraded tracker measured particles up to $|\eta| < 3$ with typical resolutions of 1.5% in p_T and 20–75 μm in the transverse impact parameter [52] for nonisolated particles of $1 < p_T < 10$ GeV. The default track selection used in CMS analyses is the “high-purity” requirement. Because low-momentum and displaced tracks share some features with nongenuine tracks such as not pointing back to the pp collision vertex and having fewer measurement points, the high-purity selection is less efficient for these tracks and so the less-restrictive “loose” requirement is often used.

Events of interest are selected using a two-tiered trigger system [53]. The first level (L1), composed of custom hardware processors, uses information from the calorimeters and muon detectors to select events at a rate of around 100 kHz within a fixed latency of about 4 μs [54]. The second level, known as the high-level trigger (HLT), consists of a farm of computing processors running a version of the full event reconstruction software optimized for fast processing, and reduces the event rate to around 1 kHz before data storage. The events used in this analysis were selected at L1 by requiring the presence of at least two muons, and at the HLT by requiring that the two muons have opposite sign (OS), with various $|\eta|$ and p_T thresholds, compatible with being produced in the dimuon decay of J/ψ or $\psi(2S)$ mesons by requiring corresponding invariant mass windows.

The PYTHIA 8.240 package [55] with the CP5 underlying event tune [56] is used to simulate the production of the Ξ_b^- and $\Xi_b(5945)^0$ states (where the Σ_b^0 baryon, with a modified mass value, is used as a proxy for the $\Xi_b(5945)^0$

state). The EvtGen 1.6.0 [57] program models the decays $\Xi_b(5945)^0 \rightarrow \Xi_b^- \pi^+$, $\Xi_b^- \rightarrow J/\psi \Xi^-$, $\Xi_b^- \rightarrow \psi(2S) \Xi^-$, $\Xi_b^- \rightarrow J/\psi \Lambda K^-$, and $\Xi_b^- \rightarrow J/\psi \Sigma^0 K^-$ with a phase-space decay model, followed by the $\psi(2S) \rightarrow \mu^+ \mu^-$, $\psi(2S) \rightarrow J/\psi \pi^+ \pi^-$, and $J/\psi \rightarrow \mu^+ \mu^-$ decays. Final-state photon radiation is included using PHOTOS 3.61 [58,59]. The generated MC events are then passed to a detailed GEANT4-based simulation [60] of the CMS detector, which includes the long-lived hyperon decays $\Xi^- \rightarrow \Lambda \pi^-$ and $\Lambda \rightarrow p \pi^-$. The simulated events are then put through the same trigger and reconstruction algorithms used for the collision data. The simulation includes effects from multiple pp interactions in the same or nearby bunch crossings (pileup) with a multiplicity distribution matching that in data.

III. EVENT RECONSTRUCTION AND SELECTION

The Ξ_b^- ground state is reconstructed using two main decay modes: $\Xi_b^- \rightarrow \psi \Xi^-$ (followed by $\psi \rightarrow \mu^+ \mu^-$), where ψ refers to the J/ψ and $\psi(2S)$ mesons, or $\Xi_b^- \rightarrow J/\psi \Lambda K^-$. We also reconstruct the decay chain $\Xi_b^- \rightarrow \psi(2S) \Xi^-$, $\psi(2S) \rightarrow J/\psi \pi^+ \pi^-$ to increase the number of events for the $\Xi_b^- \pi^+$ studies. In all the cases, the J/ψ meson is identified through its dimuon decay. The selection criteria, described below, are mainly inherited from Ref. [13].

The reconstruction chain requires two OS muons forming a good-quality vertex, passing the CMS soft-muon selection [49], and with each having $p_T(\mu) > 3$ GeV and $|\eta(\mu)| < 2.4$. To be of good quality, the fit to a dimuon common vertex must have a χ^2 vertex fit probability greater than 1%. These requirements reinforce those applied at the trigger level during the online data taking. A J/ψ or $\psi(2S)$ candidate is required to have a dimuon invariant mass within 100 MeV of the corresponding world-average mass [34], which is about 3 times the invariant mass resolution. Further, a kinematic constraint to the known ψ meson mass [34] is applied to the selected dimuon candidates.

The Λ candidates are formed from displaced two-prong vertices, assuming the decay $\Lambda \rightarrow p \pi^-$, as described in Ref. [61]. The higher-momentum track is associated with the proton and the lower-momentum track with the pion. A Λ candidate must have $p_T > 1.8$ GeV, and the $p \pi^-$ invariant mass must be within 10 MeV of the known Λ mass [34] after the tracks are refit to a common vertex, corresponding to about 3 times the invariant mass resolution. The vertex fit is then repeated with the $p \pi^-$ invariant mass constrained to the Λ mass, and its momentum recomputed. The χ^2 probability of this fit must be greater than 1%.

For the $\Xi_b^- \rightarrow \psi \Xi^-$ channel, the Ξ^- candidates are reconstructed by combining each selected Λ candidate with a charged particle track, assumed to be a pion. The

track must have $p_T > 0.3$ GeV and satisfy the loose requirement [50]. A kinematic vertex fit of the $\Xi^- \rightarrow \Lambda\pi^-$ decay is performed, and the χ^2 probability is required to be greater than 1%. The $\Lambda\pi^-$ invariant mass must be within 10 MeV of the known Ξ^- mass [34], which is about 3 times the invariant mass resolution. The resulting Ξ^- candidate must have $p_T > 2.5$ GeV. Because Λ particles mainly decay much further from the Ξ^- decay vertex than our vertex resolution, we set a requirement on the pointing angle $\alpha(\Lambda, \Xi^-)$ between the momentum of the Λ candidate and the vector from the Ξ^- decay vertex to the Λ decay vertex in the plane perpendicular to the beam direction (the transverse plane) of $\cos \alpha(\Lambda, \Xi^-) > 0.99$.

To reconstruct the decay chain $\Xi_b^- \rightarrow \psi(2S)\Xi^-$, $\psi(2S) \rightarrow J/\psi\pi^+\pi^-$, two additional OS tracks passing the high-purity requirement [50] are assigned the charged pion mass and added to the process. The higher-momentum pion must have $p_T > 0.6$ GeV, and the other pion $p_T > 0.35$ GeV. The invariant mass of the $\psi(2S)$ candidate, calculated via the formula $M(\mu^+\mu^-\pi^+\pi^-) - M(\mu^+\mu^-) + m^{\text{PDG}}(J/\psi)$, is required to be within 18 MeV of the known $\psi(2S)$ mass [34], corresponding to about 3 times the invariant mass resolution. Using this variable removes the $J/\psi \rightarrow \mu^+\mu^-$ detector invariant mass resolution from the measurement of the $M(\mu^+\mu^-\pi^+\pi^-)$ invariant mass. Here, and throughout the paper, the symbol M represents a reconstructed invariant mass and m^{PDG} the PDG world-average mass [34].

The Ξ_b^- candidates are selected by using the μ^+ , μ^- , and Ξ^- particles in a kinematic fit that constrains their momentum vectors to a common vertex and the dimuon invariant mass to the world-average J/ψ or $\psi(2S)$ mass [34]. For the decay chain $\Xi_b^- \rightarrow \psi(2S)\Xi^-$, $\psi(2S) \rightarrow J/\psi\pi^+\pi^-$, the two additional pions described above are added to the Ξ_b^- vertex fit. From all the reconstructed pp collision vertices in an event, the primary vertex (PV) is chosen as the one with the smallest pointing angle. The pointing angle is the angle between the Ξ_b^- candidate momentum and the vector joining the PV with the reconstructed Ξ_b^- candidate decay vertex. If any of the tracks used in the Ξ_b^- candidate reconstruction are included in the fit of the chosen PV, they are removed, and the PV is refit. The selected Ξ_b^- candidates are required to have $p_T(\Xi_b^-) > 10$ GeV and a χ^2 vertex fit probability greater than 1%. The pion from the $\Xi^- \rightarrow \Lambda\pi^-$ decay must satisfy an impact parameter significance requirement $d_{xy}/\sigma_{d_{xy}} > 1$, where d_{xy} is the closest distance between the track and the chosen PV in the transverse plane, and $\sigma_{d_{xy}}$ is its uncertainty. For the decay chain $\Xi_b^- \rightarrow \psi(2S)\Xi^-$, $\psi(2S) \rightarrow J/\psi\pi^+\pi^-$, we require that the two pion tracks each have $d_{xy}/\sigma_{d_{xy}} > 0.4$. The pointing angle α between the Ξ^- momentum and the vector from the Ξ_b^- decay vertex to the Ξ^- vertex in the transverse plane must satisfy $\cos \alpha(\Xi^-, \Xi_b^-) > 0.999$. The analogous angle between the

Ξ_b^- momentum and the vector from the PV to the Ξ_b^- vertex is required to have $\cos \alpha(\Xi_b^-, \text{PV}) > 0.99$. Additionally, the distance L_{xy} between the PV and the Ξ_b^- decay vertex in the transverse plane must fulfill the requirement $L_{xy}/\sigma_{L_{xy}} > 3$, where $\sigma_{L_{xy}}$ is its uncertainty.

For the $\Xi_b^- \rightarrow J/\psi\Lambda K^-$ decay channel, the J/ψ and Λ candidates are reconstructed in the same way as described above, with the additional requirement $p_T(\Lambda) > 2$ GeV. However, instead of adding a pion track to the subsequent $\Xi^- \rightarrow \Lambda\pi^-$ fit, a charged particle track with a kaon mass assignment is selected. The track must have $p_T > 1.4$ GeV and satisfy the high-purity requirement [50]. The Ξ_b^- candidates are obtained by performing a kinematic vertex fit to the μ^+ , μ^- , Λ , and K^- candidates, along with the same J/ψ mass constraint and PV selection as for the $\Xi_b^- \rightarrow \psi\Xi^-$ channel. The kaon impact parameter significance must satisfy $d_{xy}/\sigma_{d_{xy}} > 0.5$ with respect to the chosen PV. Because of the higher background in this channel more restrictive kinematic and topological requirements are applied: $p_T(\Xi_b^-) > 15$ GeV and $\cos \alpha(\Xi_b^-, \text{PV}) > 0.999$, along with the same requirements as above on the vertex fit and $L_{xy}/\sigma_{L_{xy}}$. For both the $\psi\Xi^-$ and $J/\psi\Lambda K^-$ channels, multiple Ξ_b^- candidates, found in the same event (which happens in 1%–4% of events depending on the channel) are not discarded.

Since the lifetime of the excited Ξ_b states is expected to be negligible, the $\Xi_b^-\pi^+$ candidates are formed by combining the selected Ξ_b^- candidates with each charged particle track originating from the PV and satisfying the loose requirement [50] as done in Ref. [62], which are given the charged pion mass. The pion charge must be opposite to that of the pion from $\Xi^- \rightarrow \Lambda\pi^-$ or the kaon from $\Xi_b^- \rightarrow J/\psi\Lambda K^-$. The mass difference variable $\Delta M = M(\Xi_b^-\pi^+) - M(\Xi_b^-) - m_{\pi^+}^{\text{PDG}}$ is used instead of $M(\Xi_b^-\pi^+)$ since it is characterized by a better invariant mass resolution since the effect of the Ξ_b^- invariant mass resolution is removed. From simulation studies, this variable is found to be insensitive to potential invariant mass shifts caused by the missing low-energy photon from the $\Sigma^0 \rightarrow \Lambda\gamma$ decay. As developed in Ref. [63], the Ξ_b^- candidate and all the tracks forming the PV are refit to a common vertex, further improving the $\Xi_b^-\pi^+$ invariant mass resolution from 1.07 ± 0.07 to 0.74 ± 0.04 MeV (statistical uncertainties only), as determined from simulation studies. If multiple $\Xi_b^-\pi^+$ candidates (where the multiplicity comes from the soft pion reconstruction) in an event pass the selection requirements (which happens in 10%–15% of events depending on the Ξ_b^- channel), only the highest p_T candidate is kept, which is found from simulation studies to improve the signal purity. The multiplicity estimation and a single-candidate selection is performed in the signal region of $[0, 0.06]$ GeV of the ΔM variable.

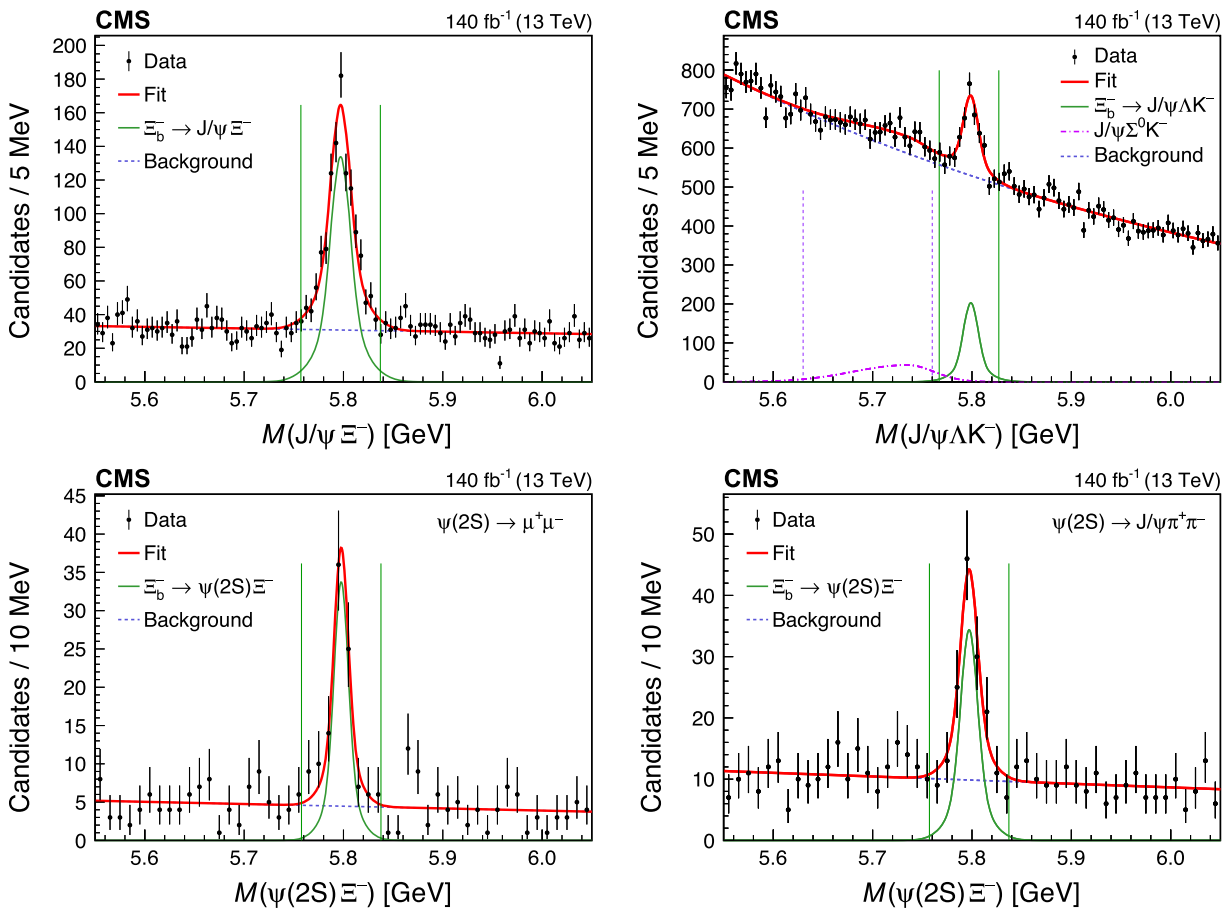


FIG. 2. Invariant mass distributions of the selected $J/\psi \Xi^-$ (upper left), $J/\psi \Lambda K^-$ (upper right), and $\psi(2S) \Xi^-$ [lower row, with $\psi(2S) \rightarrow \mu^+ \mu^-$ (left) and $\psi(2S) \rightarrow J/\psi \pi^+ \pi^-$ (right)] candidates. The data are shown by the points, while the vertical bars represent the statistical uncertainties. The overall fit result is shown by the solid red curve, with the signal and background contributions given by the solid green and dashed blue curves, respectively. The vertical lines around each peak display the mass window required for a Ξ_b^- candidate to be used in the $\Xi_b(5945)^0$ studies. The dotted-dashed curve in the upper right plot shows the fitted contribution from the $\Xi_b^- \rightarrow J/\psi \Sigma^0 K^-$ decay, with the accompanying vertical dotted lines indicating the mass window for this mode.

IV. OBSERVATION OF THE $\Xi_b^- \rightarrow \psi(2S)\Xi^-$ DECAY AND STUDIES OF THE Ξ_b^- SIGNAL

The invariant mass distributions of the selected $J/\psi \Xi^-$, $J/\psi \Lambda K^-$, and $\psi(2S) \Xi^-$ (with both $\psi(2S) \rightarrow \mu^+ \mu^-$ and $\psi(2S) \rightarrow J/\psi \pi^+ \pi^-$) candidates are shown in Fig. 2. An unbinned extended maximum likelihood fit is performed on each of these distributions. For all four channels, the signal component is described using the sum of two Gaussian functions with a common mean, whose widths and ratio between them are fixed to those determined from MC simulation. However, both widths are allowed to scale by the same free parameter in the fit to give a better description of the data. The background is described with a first-order polynomial for the $J/\psi \Xi^-$ and $\psi(2S) \Xi^-$ channels, and an exponential function for the $J/\psi \Lambda K^-$. In the latter fit, the signal contribution from the partially reconstructed $\Xi_b^- \rightarrow J/\psi \Sigma^0 K^-$ decays is taken into account by including an asymmetric Gaussian (also known as a skew normal)

function in the fit, whose shape parameters are fixed to those found from simulation studies.

The number of signal events N , the mean reconstructed Ξ_b^- invariant mass $m_{\Xi_b^-}^{\text{fit}}$, and the effective Ξ_b^- width σ_{eff} from the fit are given in Table I for each of the Ξ_b^- decay channels, along with their statistical uncertainties. The value of σ_{eff} is calculated as $\sqrt{f_1 \sigma_1^2 + (1 - f_1) \sigma_2^2}$, where σ_1 (σ_2) is the width of the first (second) Gaussian function, and f_1 is the fraction of signal events from the fit associated with the first Gaussian function. The measured resolution of the different channels is within the expectations from the available phase space and the final-state threshold proximity. The fitted Ξ_b^- mass values are consistent with the world-average value $m_{\Xi_b^-}^{\text{PDG}} = 5797.0 \pm 0.6$ MeV [34].

This is the first observation of the $\Xi_b^- \rightarrow \psi(2S)\Xi^-$ decay. Its local statistical significance is evaluated with the likelihood ratio technique, comparing the likelihood value from a fit to a signal-plus-background hypothesis to that for a

TABLE I. The number of signal events N , the mean Ξ_b^- mass $m_{\Xi_b^-}^{\text{fit}}$, and the effective Ξ_b^- width σ_{eff} from the fits to the Ξ_b^- invariant mass distributions for each of the Ξ_b^- decay channels. The uncertainties are statistical only.

Decay channel	N	$m_{\Xi_b^-}^{\text{fit}}$ (MeV)	σ_{eff} (MeV)
$\Xi_b^- \rightarrow J/\psi \Xi^-$	846 ± 40	5797.1 ± 0.6	16.3 ± 1.0
$\Xi_b^- \rightarrow J/\psi \Lambda K^-$	920 ± 98	5798.8 ± 0.9	11.9 ± 1.5
$\Xi_b^- \rightarrow J/\psi \Sigma^0 K^-$	880 ± 170
$\Xi_b^- \rightarrow \psi(2S) \Xi^-$ (with $\psi(2S) \rightarrow \mu^+ \mu^-$)	74 ± 11	5797.7 ± 1.4	11.1 ± 2.0
$\Xi_b^- \rightarrow \psi(2S) \Xi^-$ (with $\psi(2S) \rightarrow J/\psi \pi^+ \pi^-$)	90 ± 14	5797.2 ± 1.7	13.1 ± 2.8

background-only hypothesis. Since the conditions of Wilks' theorem [64] are satisfied, the asymptotic formulas of Ref. [65] [Eqs. (12) and (52)] are used to determine the $\Xi_b^- \rightarrow \psi(2S) \Xi^-$ signal significance, which is found to be well above 5 standard deviations for both the $\psi(2S) \rightarrow \mu^+ \mu^-$ and $\psi(2S) \rightarrow J/\psi \pi^+ \pi^-$ modes.

For the $\Xi_b^- \pi^+$ studies described in the next section, the Ξ_b^- candidates must have an invariant mass within 40 (30) MeV of the $m_{\Xi_b^-}^{\text{fit}}$ value for the $J/\psi \Xi^-$ and $\psi(2S) \Xi^-$ ($J/\psi \Lambda K^-$) decay channels. This corresponds to about (2.5–3) times σ_{eff} , as shown by the solid vertical lines around the peaks in Fig. 2. For the partially reconstructed $J/\psi \Sigma^0 K^-$ decay channel, a mass window of 5.63–5.76 GeV, as in Ref. [13] and shown by the vertical dotted lines in Fig. 2 (upper right), is used for the reconstructed Ξ_b^- mass.

V. STUDIES OF THE $\Xi_b(5945)^0$ BARYON

The measured ΔM distributions found by combining the selected Ξ_b^- candidates, as defined in Sec. IV, with charged particle tracks, consistent with coming from the PV and assumed to be pions, are shown in Fig. 3. The distributions are shown separately for the $\Xi_b^- \rightarrow J/\psi \Xi^-$, $\Xi_b^- \rightarrow \psi(2S) \Xi^-$ (combined $\psi(2S) \rightarrow J/\psi \pi^+ \pi^-$ and $\psi(2S) \rightarrow \mu^+ \mu^-$ modes), $\Xi_b^- \rightarrow J/\psi \Lambda K^-$, and $\Xi_b^- \rightarrow J/\psi \Sigma^0 K^-$ channels. A significant near-threshold peak is evident in all 4 distributions, in agreement with previous CMS [5] and LHCb [6,15] results. The ΔM distribution for the same-sign $\Xi_b^- \pi^-$ control sample is also displayed in Fig. 3. It shows no evidence of a peak and is consistent with the $\Xi_b^- \pi^+$ combinatorial background. No other structures are observed in this ΔM region for either the $\Xi_b^- \pi^+$ or $\Xi_b^- \pi^-$ distributions.

We fit the $\Xi_b(5945)^0$ signal using a relativistic Breit–Wigner function, which accounts for the non-negligible natural width $\Gamma(\Xi_b(5945)^0)$, convolved with a Gaussian function describing the invariant mass resolution, whose parameters are extracted from MC simulation. Lattice QCD calculations [66] give $\Gamma(\Xi_b(5945)^0) = 0.51 \pm 0.16$ MeV, the 3P_0 model predicts 0.85 MeV [67], and the latest LHCb result finds $\Gamma(\Xi_b(5945)^0) = 0.87 \pm 0.06(\text{stat}) \pm 0.05(\text{syst})$ MeV [15]. The simulation studies predict that the invariant mass resolution is slightly different for each Ξ_b^- baryon decay channel, except for the $\Xi_b^- \rightarrow J/\psi \Sigma^0 K^-$

mode, where the missing low-energy photon from the Σ^0 baryon decay produces a much wider peak with a 26% larger mass resolution. In all cases, the measured widths from the fully reconstructed decay modes are in agreement within their uncertainties.

An unbinned extended maximum likelihood simultaneous fit of all four channels is applied, where the $\Xi_b(5945)^0$ mass and natural width are constrained to be equal for all the channels, while the mass resolutions, yields, and background parameters are different. The background component is modeled with a threshold function $(\Delta M)^\alpha$, where α is a free parameter. The fit results are shown in Fig. 4, and the fitted signal yields are given in Table II.

The measured mass difference and natural width of the $\Xi_b(5945)^0$ state are $\Delta M^{\text{fit}} = 15.810 \pm 0.077$ MeV and $\Gamma(\Xi_b(5945)^0) = 0.87^{+0.22}_{-0.20}$ MeV, respectively, where the uncertainties are statistical only.

VI. EFFICIENCY AND PRODUCTION RATIO MEASUREMENTS

While in general the analysis uses events collected by a combination of different dimuon HLT paths, for the measurements of the ratios of efficiencies and the resulting branching fractions and production cross sections, a single dedicated trigger suitable for the decay topology is required in order to simplify the efficiency estimations and reduce the trigger-related systematic uncertainty. For the $\Xi_b^- \rightarrow J/\psi \Xi^-$ and $\Xi_b^- \rightarrow \psi(2S) \Xi^-$ channels, we use an inclusive dimuon HLT path, requiring the presence in the event of a J/ψ [$\psi(2S)$] meson with p_T exceeding 25 (18) GeV and decaying into two OS muons. This HLT path is only used for the 2017–2018 sample, while for the 2016 sample the similar trigger requires a minimum p_T of 20 (13) GeV for the J/ψ [$\psi(2S)$] meson. In the case of the $\Xi_b^- \rightarrow J/\psi \Lambda K^-$ channel, we use an HLT path requiring the presence of a $J/\psi \rightarrow \mu^+ \mu^-$ decay and an additional track consistent with originating from the dimuon vertex and having $d_{xy}/\sigma_{d_{xy}} > 2$. The dimuon vertex must also be displaced from the PV, by requiring $L_{xy}/\sigma_{L_{xy}} > 3$.

These requirements are much stricter than those discussed in Section III—most ψ from Ξ_b^- decays are populated within the 10–20 GeV range of p_T . Thus, using them causes a significant decrease in the signal yields for

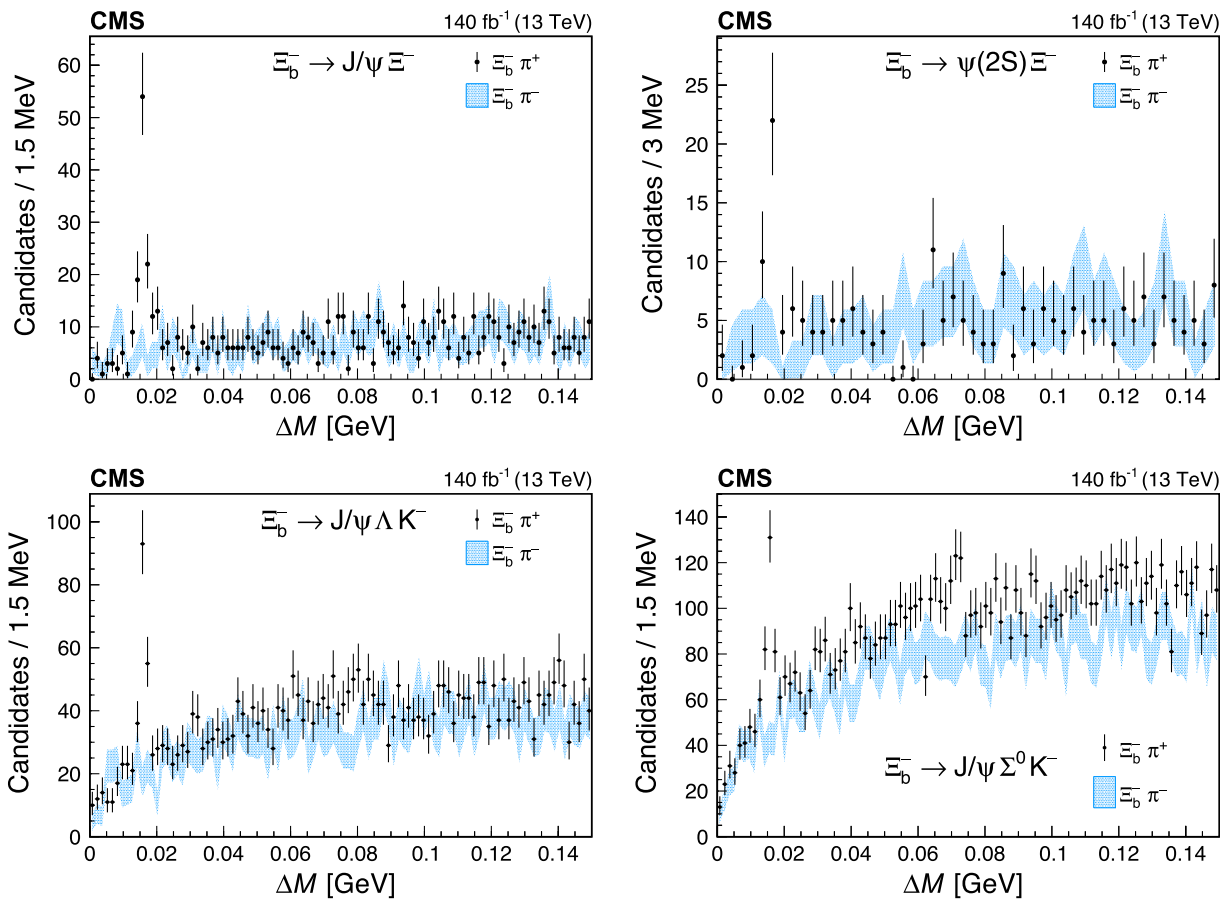


FIG. 3. The mass difference ΔM distribution of the selected $\Xi_b^- \pi^\pm$ candidates for the decay channel labeled on each plot. The points show the correct-sign combinations and the blue bands the wrong-sign. The vertical bars on the points and the length of the bands represent the statistical uncertainties in each distribution, respectively.

the $\psi\Xi^-$ channels. Redoing the fitting procedure with the new requirements leads to total signal yields of 103^{+14}_{-13} and 38^{+8}_{-7} events for $\Xi_b^- \rightarrow J/\psi\Xi^-$ and $\Xi_b^- \rightarrow \psi(2S)\Xi^-$ ($\psi(2S) \rightarrow \mu^+\mu^-$ mode), respectively. The $\Xi_b^- \rightarrow J/\psi\Lambda K^-$ signal with the tighter HLT requirement results in 606^{+67}_{-64} events. The fits to the $\Xi_b(5945)^0 \rightarrow \Xi_b^- \pi^+$ ΔM distributions are performed separately for each of the decay channels, with $\Gamma(\Xi_b(5945)^0)$ fixed to the value found from the simultaneous fit. The resulting signal yields are 13 ± 4 and 74 ± 11 events for the $J/\psi\Xi^-$ and $J/\psi\Lambda K^-$ decay modes, respectively.

TABLE II. The fitted signal yields of the $\Xi_b(5945)^0 \rightarrow \Xi_b^- \pi^+$ decay for each of the listed Ξ_b^- decay channels. Uncertainties are statistical only.

Decay channel	$N(\Xi_b(5945)^0)$
$\Xi_b^- \rightarrow J/\psi\Xi^-$	97^{+13}_{-12}
$\Xi_b^- \rightarrow \psi(2S)\Xi^-$	24^{+6}_{-5}
$\Xi_b^- \rightarrow J/\psi\Lambda K^-$	124^{+17}_{-16}
$\Xi_b^- \rightarrow J/\psi\Sigma^0 K^-$	155^{+22}_{-20}

The efficiencies for the signal and normalization channels are calculated using simulated MC samples of events that have passed the more-restrictive HLT paths described above. The total efficiency includes several factorizable contributions such as the trigger, detector acceptance, and decay channel reconstruction efficiencies. The detector acceptance term is calculated as the ratio of the number of generator-level events within the CMS kinematic acceptance to the number of generated events without any restrictions (within the full phase space region). Efficiencies for different years of data taking are estimated separately and then combined with weights corresponding to the integrated luminosity collected in each year.

Since we measure branching fractions and production cross sections with respect to normalization channels, only the ratios of such efficiencies are needed. Thus, for example, the systematic uncertainties associated with the muon, charged particle track, and Λ candidate reconstruction are reduced. Table III reports three efficiency ratios, where the first is used in measuring the quantity R , the ratio of branching fractions defined in Eq. (1), and the latter two for finding the $\Xi_b(5945)^0/\Xi_b^-$

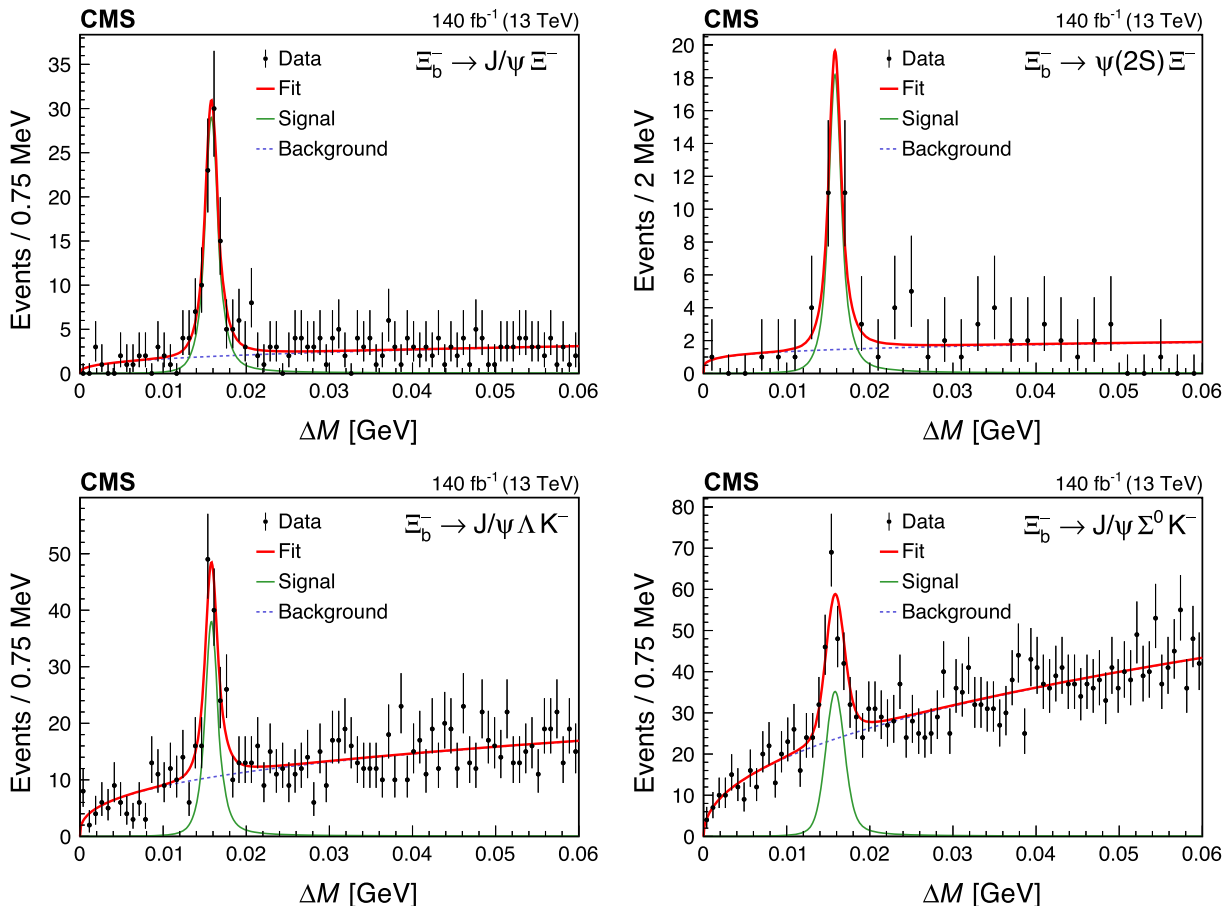


FIG. 4. Results of the simultaneous fits to the ΔM invariant mass distributions for the $\Xi_b(5945)^0$ candidates in the decay channels given in each plot. The points show the data, with the vertical bars representing the statistical uncertainty. The solid red curve displays the overall fit result, with the solid green and dashed blue curves showing the signal and background contributions, respectively.

production cross section ratio using two different decay channels: $J/\psi \Xi^-$ and $J/\psi \Lambda K^-$.

Using the measured signal yields, the efficiency ratio, and Eq. (1), we determine the ratio R of the branching fraction for the newly observed $\Xi_b^- \rightarrow \psi(2S)\Xi^-$ decay to that of the $\Xi_b^- \rightarrow J/\psi \Xi^-$ decay to be

$$R = 0.84^{+0.21}_{-0.19},$$

where the uncertainty is coming from the uncertainty in the measured yields. The uncertainty in the ratio of efficiencies is treated separately as a systematic uncertainty, as described in Sec. VII A.

Applying Eq. (2), the ratio $R_{\Xi_b(5945)^0}$ of the $\Xi_b(5945)^0$ to Ξ_b^- production is separately measured using two Ξ_b^- decay channels: $J/\psi \Xi^-$ and $J/\psi \Lambda K^-$. The results are

$$R_{\Xi_b(5945)^0}^{J/\psi \Xi^-} = 0.21 \pm 0.04$$

and

$$R_{\Xi_b(5945)^0}^{J/\psi \Lambda K^-} = 0.24 \pm 0.03,$$

where the uncertainties are statistical only (again, the efficiency uncertainties are discussed in Sec. VII A). These uncertainties account for the correlation between

TABLE III. The measured efficiency ratios and their statistical uncertainties.

Efficiency ratio	Value
$\epsilon(\Xi_b^- \rightarrow J/\psi \Xi^-)/\epsilon(\Xi_b^- \rightarrow \psi(2S)\Xi^-, \psi(2S) \rightarrow \mu^+\mu^-)$	0.304 ± 0.014
$\epsilon(\Xi_b^- \rightarrow J/\psi \Xi^-)/\epsilon(\Xi_b(5945)^0 \rightarrow \Xi_b^- \pi^+, \Xi_b^- \rightarrow J/\psi \Xi^-)$	1.645 ± 0.108
$\epsilon(\Xi_b^- \rightarrow J/\psi \Lambda K^-)/\epsilon(\Xi_b(5945)^0 \rightarrow \Xi_b^- \pi^+, \Xi_b^- \rightarrow J/\psi \Lambda K^-)$	1.941 ± 0.085

$N(\Xi_b(5945)^0)$ and $N(\Xi_b^-)$, given that the former is a subset of the latter. Both values, obtained with fully independent data and simulation samples, are in good agreement with each other and with the previous measurement by the LHCb Collaboration [6].

VII. SYSTEMATIC UNCERTAINTIES

The systematic uncertainties in the measurements given above are divided into two categories. The first is related to the uncertainties in the measured efficiency ratios and the Ξ_b^- and $\Xi_b(5945)^0$ signal yields. The second covers the uncertainties in the measured mass difference and natural width of the $\Xi_b(5945)^0$ baryon.

A. Systematic uncertainties in the measured ratios

Many systematic uncertainties related to muon reconstruction and identification, trigger effects, and efficiencies, and charged particle track and Λ candidate reconstruction cancel out in the measured ratio R due to the identical topologies of the $\Xi_b^- \rightarrow \psi(2S)\Xi^-$ and $\Xi_b^- \rightarrow J/\psi\Xi^-$ decays. There is a similar cancellation in the determination of the production cross section ratio $R_{\Xi_b(5945)^0}$, where the only topological difference between $\Xi_b(5945)^0$ and Ξ_b^- is an additional track from the $\Xi_b(5945)^0 \rightarrow \Xi_b^- \pi^+$ decay.

The systematic uncertainty related to the choice of fit functions used to describe the signal and background shapes in the invariant mass fits is evaluated by varying the functions used and recording the change in the number of signal events. For the three Ξ_b^- decay channels, we first perform the fit with the resolution scaling parameter for the sum of the two Gaussian functions set to unity and note the change in the fit results. We then use a Student's t distribution [68] to model the signal, with the mean and width allowed to be free and the n parameter (corresponding to the number of degrees of freedom) fixed from the simulation. This function, being symmetric and bell-shaped, also models a heavy-tailed distribution and thus is found to be a reliable alternative to the sum of two Gaussian functions. A single Gaussian function with free parameters is also tried for fitting the $\psi(2S)\Xi^-$ and $J/\psi\Xi^-$ signals. Using the largest change in the number of events, the resulting systematic uncertainty in R from this source is 8.8%.

Two alternative background functions are considered in fitting the $J/\psi\Xi^-$ and $\psi(2S)\Xi^-$ invariant mass distributions: an exponential function and a second-order polynomial. For the more complicated background shape in the $J/\psi\Lambda K^-$ distribution, we switch from an exponential function to a second-order polynomial. The resulting systematic uncertainty in R from this source is estimated as 4.5%. The combined signal-plus-background Ξ_b^- fit model uncertainties are estimated as 4.0 and 6.9% in the $R_{\Xi_b(5945)^0}^{J/\psi\Xi^-}$ and $R_{\Xi_b(5945)^0}^{J/\psi\Lambda K^-}$ values, respectively.

The alternative functions used in fitting the $\Xi_b(5945)^0 \rightarrow \Xi_b^- \pi^+$ ΔM distribution are described in the next subsection when the systematic uncertainties in the measured $\Xi_b(5945)^0$ mass and width are discussed. The resulting systematic uncertainties due to the fitting functions in the $R_{\Xi_b(5945)^0}$ production cross section ratio are 7.7 and 6.7% for the $J/\psi\Xi^-$ and $J/\psi\Lambda K^-$ decay modes, respectively.

For the R measurement, given that we are using different HLT paths for the $\Xi_b^- \rightarrow J/\psi\Xi^-$ and the $\Xi_b^- \rightarrow \psi(2S)\Xi^-$ signals, a cross-check of the correctness and robustness of such a procedure is performed. The similar branching fraction ratio $R_{B^+} = \mathcal{B}(B^+ \rightarrow \psi(2S)K^+)/\mathcal{B}(B^+ \rightarrow J/\psi K^+)$ was measured with the triggers we use for the Ξ_b^- signals, and the resulting value of 0.601 ± 0.030 is consistent with the world-average value [34] 0.605 ± 0.021 . The 5% precision of the R_{B^+} value is taken conservatively as an additional systematic uncertainty in the R measurement.

As mentioned above, an additional source of uncertainty in the $R_{\Xi_b(5945)^0}$ measurement comes from identifying the extra pion in the $\Xi_b(5945)^0 \rightarrow \Xi_b^- \pi^+$ decay. The uncertainty in the tracking reconstruction efficiency for the low- p_T pion is estimated as 5.2% [69].

The uncertainty related to the finite size of the MC samples is also considered as a systematic uncertainty. It is estimated from the statistical uncertainty in the determinations of the efficiency ratios from the MC simulation. This corresponds to a systematic uncertainty of 4.6% in R , and 6.5 and 4.4% in $R_{\Xi_b(5945)^0}$ for the $J/\psi\Xi^-$ and $J/\psi\Lambda K^-$ modes, respectively.

The systematic uncertainties in the R and $R_{\Xi_b(5945)^0}$ measurements are summarized in Tables IV and V, respectively, along with the total systematic uncertainties, calculated from the sum in quadrature of the individual sources.

B. Systematic uncertainties in the $\Xi_b(5945)^0$ baryon mass and width measurements

Several sources of systematic uncertainty are considered in the simultaneous measurement of the $\Xi_b(5945)^0$ baryon mass difference and natural width. To evaluate the systematic uncertainties related to the choice of functions used to fit the $\Xi_b(5945)^0$ ΔM distributions, alternative functions are chosen and the maximum changes in the results of the fit are used to estimate the corresponding systematic

TABLE IV. Systematic uncertainties in percent in the ratio R from the different sources and the total uncertainty.

Source	Uncertainty (%)
Signal model	8.8
Background model	4.5
R_{B^+} uncertainty	5.0
MC finite size	4.6
Total	12.0

TABLE V. Systematic uncertainties in percent in the ratio $R_{\Xi_b(5945)^0}$ from the different sources and the total uncertainty, separately for the $J/\psi \Xi^-$ and $J/\psi \Lambda K^-$ decay modes.

Source	$J/\psi \Xi^-$ (%)	$J/\psi \Lambda K^-$ (%)
Ξ_b^- fit model	4.0	6.9
$\Xi_b(5945)^0$ fit model	7.7	6.7
Tracking efficiency	5.2	5.2
MC finite size	6.5	4.4
Total	12.0	11.8

uncertainty. We use a Student's t-distribution [68] as the alternative function to describe the invariant mass resolution, with the shape parameters determined from MC simulation. Fitting the data distributions leads to estimates for the systematic uncertainty of ± 0.003 MeV in the mass difference, while the change in the natural width is negligible.

We also vary the function used to describe the background in the fit. We use the threshold function described earlier, multiplied by a first-order polynomial, except for the $\Xi_b^- \rightarrow \psi(2S)\Xi^-$ decay channel, where the number of events is too small to allow a reasonable fit to the background for functions with more parameters. Another alternative model uses the baseline background model to fit the same-sign $\Xi_b^- \pi^-$ distributions. The α values obtained in these fits are then used as fixed parameters of the simultaneous fit. From this, we estimate systematic uncertainties from this source of ± 0.002 and ± 0.04 MeV in the mass difference and natural width, respectively.

The systematic uncertainty coming from the choice of the fit range is estimated by varying the ΔM fit region from [0, 0.05] to [0, 0.09] GeV. The maximum deviation of the fit parameters is used as the systematic uncertainty, giving ± 0.023 and ± 0.13 MeV in the mass difference and natural width, respectively.

The signal shape for the $\Xi_b(5945)^0$ ΔM distribution is fit with a Gaussian resolution function, convolved with a relativistic Breit–Wigner (RBW) and a Blatt–Weisskopf barrier factor [70], with the radial parameter in these functions set to $r = 3.5$ GeV $^{-1}$ and the angular momentum (spin) to $\ell = 1$. To determine the systematic uncertainty associated with these choices, the fit is repeated with the value of r varied in the range 1–5 GeV $^{-1}$ and ℓ set to 0 or 2. The change in r has a negligible effect, while the spin change leads to systematic uncertainties of ± 0.022 and ± 0.02 MeV in the mass difference and natural width measurements, respectively.

For the $\Xi_b^- \rightarrow J/\psi \Xi^-$ channel, we verify that the mass resolutions obtained in data and simulation agree to within the combined uncertainty of 7.5%. We obtain a systematic uncertainty associated with any potential disagreement in the ΔM mass resolution between data and simulation by repeating the $\Xi_b(5945)^0$ fit with the resolutions from MC

TABLE VI. The systematic uncertainties in MeV in the measurement of the $\Xi_b(5945)^0$ mass difference and natural width from each of the sources, along with the total uncertainties.

Source	ΔM (MeV)	$\Gamma(\Xi_b(5945)^0)$ (MeV)
Signal model	0.003	< 0.01
Background model	0.002	0.04
Fit range	0.023	0.13
RBW shape	0.022	0.02
Mass resolution	0.004	0.08
Shift from reconstruction	0.041	...
Total	0.052	0.16

scaled up or down by 1.075. The resulting systematic uncertainties are ± 0.004 and ± 0.08 MeV for the mass difference and natural width, respectively.

Simulation studies show a shift of 0.041 MeV between the reconstructed and generated mass differences for the $\Xi_b(5945)^0$ baryon peak; this shift is treated as an additional systematic uncertainty in the ΔM^{fit} measurement.

The systematic uncertainties described above are summarized in Table VI, together with the total systematic uncertainties, found from the sum in quadrature of those from the individual sources.

VIII. RESULTS

Our final result for the ratio of the branching fractions for the $\Xi_b^- \rightarrow \psi(2S)\Xi^-$ decay with respect to the $\Xi_b^- \rightarrow J/\psi \Xi^-$ normalization mode is

$$R = \frac{\mathcal{B}(\Xi_b^- \rightarrow \psi(2S)\Xi^-)}{\mathcal{B}(\Xi_b^- \rightarrow J/\psi \Xi^-)} \\ = 0.84^{+0.21}_{-0.19}(\text{stat}) \pm 0.10(\text{syst}) \pm 0.02(\mathcal{B}),$$

where the uncertainties are statistical, systematic, and related to the uncertainties in the J/ψ and $\psi(2S)$ branching fractions, respectively. For the last term of Eq. (1), we used the lepton universality assumption of $\mathcal{B}(J/\psi \rightarrow \mu^+\mu^-)/\mathcal{B}(\psi(2S) \rightarrow \mu^+\mu^-) = \mathcal{B}(J/\psi \rightarrow e^+e^-)/\mathcal{B}(\psi(2S) \rightarrow e^+e^-) = 7.53 \pm 0.17$ from the PDG [34], since the dielectron modes are measured more precisely than the dimuon ones.

Including the systematic uncertainties described in the previous section, the $\Xi_b(5945)^0$ mass difference and natural width are found to be

$$\mathcal{M}(\Xi_b(5945)^0) - \mathcal{M}(\Xi_b^-) - m^{\text{PDG}}(\pi^\pm) \\ = 15.810 \pm 0.077(\text{stat}) \pm 0.052(\text{syst}) \text{ MeV},$$

$$\Gamma(\Xi_b(5945)^0) = 0.87^{+0.22}_{-0.20}(\text{stat}) \pm 0.16(\text{syst}) \text{ MeV}.$$

Using the world-average Ξ_b^- baryon mass [34], our ΔM^{fit} value corresponds to a $\Xi_b(5945)^0$ mass of $5952.4 \pm 0.1(\text{stat+syst}) \pm 0.6(m_{\Xi_b^-})$ MeV, where the first uncertainty includes the statistical and systematic components

and the last comes from the uncertainty in the Ξ_b^- mass. These measurements of the $\Xi_b(5945)^0$ baryon mass and width are significantly more precise than the previous CMS results [5] and in agreement with those obtained by the LHCb experiment [6,15]. Their recent measurement, using data corresponding to an integrated luminosity of 9 fb^{-1} , reported $\Delta M = 15.80 \pm 0.02 \pm 0.01 \text{ MeV}$ and $\Gamma(\Xi_b(5945)^0) = 0.87 \pm 0.06 \pm 0.05 \text{ MeV}$ [15].

Finally, our measurement of the inclusive ratio of the $\Xi_b(5945)^0$ and Ξ_b^- production cross sections gives

$$R_{\Xi_b(5945)^0} = \frac{\sigma(pp \rightarrow \Xi_b(5945)^0 X) \mathcal{B}(\Xi_b(5945)^0 \rightarrow \Xi_b^- \pi^+)}{\sigma(pp \rightarrow \Xi_b^- X)} \\ = 0.22 \pm 0.02(\text{stat}) \pm 0.02(\text{syst}),$$

where we used the BLUE procedure [71–73] to combine the results from the $\Xi_b^- \rightarrow J/\psi \Xi^-$ and $\Xi_b^- \rightarrow J/\psi \Lambda K^-$ decay modes. The statistical and systematic uncertainties are assumed to be uncorrelated, except for the tracking efficiency, which we treat as correlated.

IX. SUMMARY AND CONCLUSIONS

In this article, we present the first observation of the $\Xi_b^- \rightarrow \psi(2S)\Xi^-$ decay. We use data from LHC proton-proton (pp) collisions at $\sqrt{s} = 13 \text{ TeV}$, collected by the CMS experiment during 2016–2018, corresponding to an integrated luminosity of 140 fb^{-1} . We measure the ratio of the branching fraction for the new decay to that for $\Xi_b^- \rightarrow J/\psi \Xi^-$ to be

$$R = \frac{\mathcal{B}(\Xi_b^- \rightarrow \psi(2S)\Xi^-)}{\mathcal{B}(\Xi_b^- \rightarrow J/\psi \Xi^-)} \\ = 0.84^{+0.21}_{-0.19}(\text{stat}) \pm 0.10(\text{syst}) \pm 0.02(\mathcal{B}),$$

where the last uncertainty comes from the uncertainties in the J/ψ and $\psi(2S)$ branching fractions.

This result is consistent with analogous measured ratios from $B_{(s)}$ and Λ_b^0 decays such as $B^+ \rightarrow \psi K^+$, $B^0 \rightarrow \psi K_s^0$, $B_s^0 \rightarrow \psi \phi$, and $\Lambda_b^0 \rightarrow \psi \Lambda$, whose values are in the range 0.5–0.6 [34] (here ψ refers to the J/ψ and $\psi(2S)$ mesons). In general, currently existing results for such ratios do not form any clear and unambiguous pattern. New measurements, such as the one reported here, and corresponding theoretical predictions are required to build a robust model that can reliably describe b hadron decays to charmonium states.

We reconstruct $\Xi_b(5945)^0$ candidates using the $\Xi_b(5945)^0 \rightarrow \Xi_b^- \pi^+$ decay mode by combining tracks from the pp collision vertex with Ξ_b^- candidates from four different decay modes. A simultaneous fit of all decay modes is used to extract the mass difference and natural width, which are consistent with our previous results [5], but with much better precision. They are also in agreement

with the LHCb measurements [6,15]. Using the world-average value for the Ξ_b^- baryon mass [34], we measure the mass of the $\Xi_b(5945)^0$ baryon to be

$$M(\Xi_b(5945)^0) = 5952.4 \pm 0.1(\text{stat + syst}) \\ \pm 0.6(m_{\Xi_b^-}) \text{ MeV},$$

where the last uncertainty comes from the uncertainty in the Ξ_b^- baryon mass. We measure the natural width to be $\Gamma(\Xi_b(5945)^0) = 0.87^{+0.22}_{-0.20}(\text{stat}) \pm 0.16(\text{syst}) \text{ MeV}$.

Finally, our determination of the $\Xi_b(5945)^0/\Xi_b^-$ relative production rate $R_{\Xi_b(5945)^0} = 0.22 \pm 0.02(\text{stat}) \pm 0.02(\text{syst})$ is in good agreement with the LHCb result [6] of $0.28 \pm 0.03 \pm 0.01$ and is of a similar precision. From the measured values of this ratio, we conclude that about 1/4 of Ξ_b^- baryons are produced from the $\Xi_b(5945)^0 \rightarrow \Xi_b^- \pi^+$ decay. The other major $\Xi_b(5945)^0$ decay is $\Xi_b(5945)^0 \rightarrow \Xi_b^0 \pi^0$. Since $\mathcal{B}(\Xi_b^* \rightarrow \Xi_b \pi)$ should be close to 100%, we expect $\mathcal{B}(\Xi_b(5945)^0 \rightarrow \Xi_b^- \pi^+) \approx 2\mathcal{B}(\Xi_b(5945)^0 \rightarrow \Xi_b^0 \pi^0) \approx 2/3$, where the factor of 2 comes from isospin differences and the Clebsch-Gordan coefficients [34]. Incorporating this estimate of $\mathcal{B}(\Xi_b(5945)^0 \rightarrow \Xi_b^- \pi^+)$ into our results for the ratio of production cross sections, we find that $\sigma(pp \rightarrow \Xi_b(5945)^0 X)/\sigma(pp \rightarrow \Xi_b^- X) \approx 1/3$. If the relative production rate for Ξ_b^{*-} to Ξ_b^- follows the same scheme, the corresponding ratio can be estimated as $R_{\Xi_b^{*-}} = [\sigma(pp \rightarrow \Xi_b^{*-} X) \mathcal{B}(\Xi_b^{*-} \rightarrow \Xi_b^- \pi^0)]/\sigma(pp \rightarrow \Xi_b^- X) \approx 1/3 \times 1/3 = 1/9$. Thus, we can conclude that about a third of the Ξ_b^- baryons are produced from Ξ_b^* decays.

Since decays from higher-mass excited Ξ_b baryons are also possible, such as the $\Xi_b(6227)$ doublet reported by the LHCb experiment [11,12], less than two thirds of the Ξ_b^- baryons are expected to be directly produced from pp collisions. It is clear that further studies of different ground- and excited-state Ξ_b baryons are needed to fully understand this family of baryons.

ACKNOWLEDGMENTS

We congratulate our colleagues in the CERN accelerator departments for the excellent performance of the LHC and thank the technical and administrative staffs at CERN and at other CMS institutes for their contributions to the success of the CMS effort. In addition, we gratefully acknowledge the computing centers and personnel of the Worldwide LHC Computing Grid and other centers for delivering so effectively the computing infrastructure essential to our analyses. Finally, we acknowledge the enduring support for the construction and operation of the LHC, the CMS detector, and the supporting computing infrastructure provided by the following funding agencies: SC (Armenia), BMBWF and FWF (Austria); FNRS and FWO (Belgium); CNPq, CAPES, FAPERJ, FAPERGS, and FAPESP

(Brazil); MES and BNSF (Bulgaria); CERN; CAS, MoST, and NSFC (China); MINCIENCIAS (Colombia); MSES and CSF (Croatia); RIF (Cyprus); SENESCYT (Ecuador); ERC PRG, RVTT3 and MoER TK202 (Estonia); Academy of Finland, MEC, and HIP (Finland); CEA and CNRS/IN2P3 (France); SRNSF (Georgia); BMBF, DFG, and HGF (Germany); GSRI (Greece); NKFH (Hungary); DAE and DST (India); IPM (Iran); SFI (Ireland); INFN (Italy); MSIP and NRF (Republic of Korea); MES (Latvia); LMTLT (Lithuania); MOE and UM (Malaysia); BUAP, CINVESTAV, CONACYT, LNS, SEP, and UASLP-FAI (Mexico); MOS (Montenegro); MBIE (New Zealand); PAEC (Pakistan); MES and NSC (Poland); FCT (Portugal); MESTD (Serbia); MCIN/AEI and PCTI (Spain); MOSTR (Sri Lanka); Swiss Funding Agencies (Switzerland); MST (Taipei); MHESI and NSTDA (Thailand); TUBITAK and TENMAK (Turkey); NASU (Ukraine); STFC (United Kingdom); DOE and NSF (USA). Individuals have received support from the Marie-Curie program and the European Research Council and Horizon 2020 Grant, contract Nos. 675440, 724704, 752730, 758316, 765710, 824093, 101115353, and COST Action CA16108 (European Union); the Leventis Foundation; the Alfred P. Sloan Foundation; the Alexander von Humboldt Foundation; the Science Committee, project no. 22rl-037 (Armenia); the Belgian Federal Science Policy Office; the Fonds pour la Formation à la Recherche dans l’Industrie et dans l’Agriculture (FRIA-Belgium); the Agentschap voor Innovatie door Wetenschap en Technologie (IWT-Belgium); the F.R.S.-FNRS and FWO (Belgium) under the “Excellence of Science—EOS”—be.h project n. 30820817; the Beijing Municipal Science & Technology Commission, No. Z191100007219010 and Fundamental Research Funds for the Central Universities (China); the Ministry of Education, Youth and Sports (MEYS) of the Czech

Republic; the Shota Rustaveli National Science Foundation, grant No. FR-22-985 (Georgia); the Deutsche Forschungsgemeinschaft (DFG), under Germany’s Excellence Strategy—EXC 2121 “Quantum Universe”—390833306, and under project number 400140256–GRK2497; the Hellenic Foundation for Research and Innovation (HFRI), Project Number 2288 (Greece); the Hungarian Academy of Sciences, the New National Excellence Program—ÚNKP, the NKFH research grants No. K 124845, No. K 124850, No. K 128713, No. K 128786, No. K 129058, No. K 131991, No. K 133046, No. K 138136, No. K 143460, No. K 143477, No. 2020-2.2.1-ED-2021-00181, and No. TKP2021-NKTA-64 (Hungary); the Council of Science and Industrial Research, India; ICS—National Research Center for High Performance Computing, Big Data and Quantum Computing, funded by the EU NextGeneration program (Italy); the Latvian Council of Science; the Ministry of Education and Science, project no. 2022/WK/14, and the National Science Center, contracts Opus No. 2021/41/B/ST2/01369 and No. 2021/43/B/ST2/01552 (Poland); the Fundação para a Ciência e a Tecnologia, grant No. CEECIND/01334/2018 (Portugal); the National Priorities Research Program by Qatar National Research Fund; MCIN/AEI/10.13039/501100011033, ERDF “a way of making Europe”, and the Programa Estatal de Fomento de la Investigación Científica y Técnica de Excelencia María de Maeztu, Grant No. MDM-2017-0765 and Programa Severo Ochoa del Principado de Asturias (Spain); the Chulalongkorn Academic into Its 2nd Century Project Advancement Project, and the National Science, Research and Innovation Fund via the Program Management Unit for Human Resources & Institutional Development, Research and Innovation, grant No. B37G660013 (Thailand); the Kavli Foundation; the Nvidia Corporation; the SuperMicro Corporation; the Welch Foundation, contract No. C-1845; and the Weston Havens Foundation (USA).

-
- [1] D. Ebert, T. Feldmann, C. Kettner, and H. Reinhardt, A diquark model for baryons containing one heavy quark, *Z. Phys. C* **71**, 329 (1996).
 - [2] V. M. Abazov *et al.* (D0 Collaboration), Direct observation of the strange b baryon Ξ_b^- , *Phys. Rev. Lett.* **99**, 052001 (2007).
 - [3] T. Aaltonen *et al.* (CDF Collaboration), Observation and mass measurement of the baryon Ξ_b^- , *Phys. Rev. Lett.* **99**, 052002 (2007).
 - [4] T. Aaltonen *et al.* (CDF Collaboration), Observation of the Ξ_b^0 baryon, *Phys. Rev. Lett.* **107**, 102001 (2011).
 - [5] CMS Collaboration, Observation of a new Ξ_b baryon, *Phys. Rev. Lett.* **108**, 252002 (2012).
 - [6] LHCb Collaboration, Measurement of the properties of the Ξ_b^{*0} baryon, *J. High Energy Phys.* **05** (2016) 161.
 - [7] LHCb Collaboration, Observation of two new Ξ_b^- baryon resonances, *Phys. Rev. Lett.* **114**, 062004 (2015).
 - [8] E. E. Jenkins, Model-independent bottom baryon mass predictions in the $1/N_c$ expansion, *Phys. Rev. D* **77**, 034012 (2008).
 - [9] M. Karliner, B. Keren-Zur, H. J. Lipkin, and J. L. Rosner, The quark model and b baryons, *Ann. Phys. (Amsterdam)* **324**, 2 (2009).
 - [10] D. Ebert, R. N. Faustov, and V. O. Galkin, Masses of excited heavy baryons in the relativistic quark model, *Phys. Lett. B* **659**, 612 (2008).

- [11] LHCb Collaboration, Observation of a new Ξ_b^- resonance, *Phys. Rev. Lett.* **121**, 072002 (2018).
- [12] LHCb Collaboration, Observation of a new Ξ_b^0 state, *Phys. Rev. D* **103**, 012004 (2021).
- [13] CMS Collaboration, Observation of a new excited beauty strange baryon decaying to $\Xi_b^-\pi^+\pi^-$, *Phys. Rev. Lett.* **126**, 252003 (2021).
- [14] LHCb Collaboration, Observation of two new excited Ξ_b^0 states decaying to $\Lambda_b^0 K^-\pi^+$, *Phys. Rev. Lett.* **128**, 162001 (2022).
- [15] LHCb Collaboration, Observation of new baryons in the $\Xi_b^-\pi^+\pi^-$ and $\Xi_b^0\pi^+\pi^-$ systems, *Phys. Rev. Lett.* **131**, 171901 (2023).
- [16] W. Roberts and M. Pervin, Heavy baryons in a quark model, *Int. J. Mod. Phys. A* **23**, 2817 (2008).
- [17] D. Ebert, R. N. Faustov, and V. O. Galkin, Spectroscopy and Regge trajectories of heavy baryons in the relativistic quark-diquark picture, *Phys. Rev. D* **84**, 014025 (2011).
- [18] H. Garcilazo, J. Vijande, and A. Valcarce, Faddeev study of heavy baryon spectroscopy, *J. Phys. G* **34**, 961 (2007).
- [19] B. Chen, K.-W. Wei, and A. Zhang, Assignments of Λ_Q and Ξ_Q baryons in the heavy quark-light diquark picture, *Eur. Phys. J. A* **51**, 82 (2015).
- [20] I. L. Grach, I. M. Narodetskii, M. A. Trusov, and A. I. Veselov, Heavy baryon spectroscopy in the QCD string model, in *Particles and Nuclei. Proceedings, 18th International Conference, PANIC08, Eilat, Israel* (2008), arXiv:0811.2184.
- [21] Q. Mao, H.-X. Chen, W. Chen, A. Hosaka, X. Liu, and S.-L. Zhu, QCD sum rule calculation for P-wave bottom baryons, *Phys. Rev. D* **92**, 114007 (2015).
- [22] Z.-G. Wang, Analysis of the $1/2^-$ and $3/2^-$ heavy and doubly heavy baryon states with QCD sum rules, *Eur. Phys. J. A* **47**, 81 (2011).
- [23] K.-L. Wang, Y.-X. Yao, X.-H. Zhong, and Q. Zhao, Strong and radiative decays of the low-lying S - and P -wave singly heavy baryons, *Phys. Rev. D* **96**, 116016 (2017).
- [24] Y. Kawakami and M. Harada, Singly heavy baryons with chiral partner structure in a three-flavor chiral model, *Phys. Rev. D* **99**, 094016 (2019).
- [25] Z.-Y. Wang, J.-J. Qi, X.-H. Guo, and K.-W. Wei, Spectra of charmed and bottom baryons with hyperfine interaction, *Chin. Phys. C* **41**, 093103 (2017).
- [26] K. Thakkar, Z. Shah, A. K. Rai, and P. C. Vinodkumar, Excited state mass spectra and Regge trajectories of bottom baryons, *Nucl. Phys. A* **965**, 57 (2017).
- [27] K.-W. Wei, B. Chen, N. Liu, Q.-Q. Wang, and X.-H. Guo, Spectroscopy of singly, doubly, and triply bottom baryons, *Phys. Rev. D* **95**, 116005 (2017).
- [28] LHCb Collaboration, Studies of beauty baryon decays to $D^0\phi^-$ and $\Lambda_c^+ h^-$ final states, *Phys. Rev. D* **89**, 032001 (2014).
- [29] LHCb Collaboration, Evidence for the strangeness-changing weak decay $\Xi_b^- \rightarrow \Lambda_b^0\pi^-$, *Phys. Rev. Lett.* **115**, 241801 (2015).
- [30] LHCb Collaboration, Observation of the decay $\Xi_b^- \rightarrow pK^-K^-$, *Phys. Rev. Lett.* **118**, 071801 (2017).
- [31] LHCb Collaboration, Observation of the $\Xi_b^- \rightarrow J/\psi\Lambda K^-$ decay, *Phys. Lett. B* **772**, 265 (2017).
- [32] LHCb Collaboration, Measurement of branching fractions of charmless four-body Λ_b^0 and Ξ_b^0 decays, *J. High Energy Phys.* **02** (2018) 098.
- [33] LHCb Collaboration, Isospin amplitudes in $\Lambda_b^0 \rightarrow J/\psi\Lambda(\Sigma^0)$ and $\Xi_b^0 \rightarrow J/\psi\Xi^0(\Lambda)$ decays, *Phys. Rev. Lett.* **124**, 111802 (2020).
- [34] Particle Data Group, Review of particle physics, *Prog. Theor. Exp. Phys.* **2022**, 083C01 (2022).
- [35] LHCb Collaboration, Evidence of a $J/\psi\Lambda$ structure and observation of excited Ξ^- states in the $\Xi_b^- \rightarrow J/\psi\Lambda K^-$ decay, *Sci. Bull.* **66**, 1278 (2021).
- [36] LHCb Collaboration, Search for CP violation in $\Xi_b^- \rightarrow pK^-K^-$ decays, *Phys. Rev. D* **104**, 052010 (2021).
- [37] A. G. Grozin, *Heavy Quark Effective Theory* (Springer, Berlin, Heidelberg, 2004), p. 1, 10.1007/b79301.
- [38] N. Isgur and M. B. Wise, Spectroscopy with heavy quark symmetry, *Phys. Rev. Lett.* **66**, 1130 (1991).
- [39] M. A. Shifman and M. B. Voloshin, Preasymptotic effects in inclusive weak decays of charmed particles, *Sov. J. Nucl. Phys.* **41**, 120 (1985).
- [40] N. Isgur and M. B. Wise, Weak decays of heavy mesons in the static quark approximation, *Phys. Lett. B* **232**, 113 (1989).
- [41] I. I. Y. Bigi, N. G. Uraltsev, and A. I. Vainshtein, Non-perturbative corrections to inclusive beauty and charm decays: QCD versus phenomenological models, *Phys. Lett. B* **293**, 430 (1992); **297**, 477(E) (1992).
- [42] CMS Collaboration, Precision luminosity measurement in proton-proton collisions at $\sqrt{s} = 13$ TeV in 2015 and 2016 at CMS, *Eur. Phys. J. C* **81**, 800 (2021).
- [43] CMS Collaboration, CMS luminosity measurement for the 2017 data-taking period at $\sqrt{s} = 13$ TeV, CMS Physics Analysis Summary, Report No. CMS-PAS-LUM-17-004, 2018, <https://cds.cern.ch/record/2621960>.
- [44] CMS Collaboration, CMS luminosity measurement for the 2018 data-taking period at $\sqrt{s} = 13$ TeV, CMS Physics Analysis Summary CMS-PAS-LUM-18-002, 2019, <https://cds.cern.ch/record/2676164>.
- [45] CMS Collaboration, Measurement of $B_c(2s)^+$ and $B_c^*(2S)^+$ cross section ratios in proton-proton collisions at $\sqrt{s} = 13$ TeV, *Phys. Rev. D* **102**, 092007 (2020).
- [46] HEPData record for this analysis (2024), 10.17182/hepdata.146756.
- [47] CMS Collaboration, The CMS experiment at the CERN LHC, *J. Instrum.* **3**, S08004 (2008).
- [48] CMS Collaboration, Development of the CMS detector for the CERN LHC run 3, *J. Instrum.* **19**, P05064 (2024).
- [49] CMS Collaboration, Performance of the CMS muon detector and muon reconstruction with proton-proton collisions at $\sqrt{s} = 13$ TeV, *J. Instrum.* **13**, P06015 (2018).
- [50] CMS Collaboration, Description and performance of track and primary-vertex reconstruction with the CMS tracker, *J. Instrum.* **9**, P10009 (2014).
- [51] CMS Tracker Group, The CMS Phase-1 pixel detector upgrade, *J. Instrum.* **16**, P02027 (2021).
- [52] CMS Collaboration, Track impact parameter resolution for the full pseudorapidity coverage in the 2017 dataset with the CMS Phase-1 Pixel detector, CMS Detector Performance Note CMS-DP-2020-049, 2020, <https://cds.cern.ch/record/2743740>.

- [53] CMS Collaboration, The CMS trigger system, *J. Instrum.* **12**, P01020 (2017).
- [54] CMS Collaboration, Performance of the CMS level-1 trigger in proton-proton collisions at $\sqrt{s} = 13$ TeV, *J. Instrum.* **15**, P10017 (2020).
- [55] T. Sjöstrand, S. Ask, J. R. Christiansen, R. Corke, N. Desai, P. Ilten, S. Mrenna, S. Prestel, C. O. Rasmussen, and P. Z. Skands, An introduction to PYTHIA 8.2, *Comput. Phys. Commun.* **191**, 159 (2015).
- [56] CMS Collaboration, Extraction and validation of a new set of CMS PYTHIA8 tunes from underlying-event measurements, *Eur. Phys. J. C* **80**, 4 (2020).
- [57] D. J. Lange, The EVTGEN particle decay simulation package, *Nucl. Instrum. Methods Phys. Res., Sect. A* **462**, 152 (2001).
- [58] E. Barberio, B. van Eijk, and Z. Wąs, PHOTOS: A universal Monte Carlo for QED radiative corrections in decays, *Comput. Phys. Commun.* **66**, 115 (1991).
- [59] E. Barberio and Z. Wąs, PHOTOS: A universal Monte Carlo for QED radiative corrections. version 2.0, *Comput. Phys. Commun.* **79**, 291 (1994).
- [60] S. Agostinelli *et al.* (GEANT4 Collaboration), GEANT4—a simulation toolkit, *Nucl. Instrum. Methods Phys. Res., Sect. A* **506**, 250 (2003).
- [61] CMS Collaboration, CMS tracking performance results from early LHC operation, *Eur. Phys. J. C* **70**, 1165 (2010).
- [62] CMS Collaboration, Observation of two excited B_c^+ states and measurement of the $B_c^+(2S)$ mass in pp collisions at $\sqrt{s} = 13$ TeV, *Phys. Rev. Lett.* **122**, 132001 (2019).
- [63] CMS Collaboration, Study of excited Λ_b^0 states decaying to $\Lambda_b^0\pi^+\pi^-$ in proton-proton collisions at $\sqrt{s} = 13$ TeV, *Phys. Lett. B* **803**, 135345 (2020).
- [64] S. S. Wilks, The large-sample distribution of the likelihood ratio for testing composite hypotheses, *Ann. Math. Stat.* **9**, 60 (1938).
- [65] G. Cowan, K. Cranmer, E. Gross, and O. Vitells, Asymptotic formulae for likelihood-based tests of new physics, *Eur. Phys. J. C* **71**, 1554 (2011); **73**, 2501(E) (2013).
- [66] W. Detmold, C.-J. D. Lin, and S. Meinel, Calculation of the heavy-hadron axial couplings g_1 , g_2 and g_3 using lattice QCD, *Phys. Rev. D* **85**, 114508 (2012).
- [67] C. Chen, X.-L. Chen, X. Liu, W.-Z. Deng, and S.-L. Zhu, Strong decays of charmed baryons, *Phys. Rev. D* **75**, 094017 (2007).
- [68] S. Jackman, *Bayesian Analysis for the Social Sciences* (John Wiley & Sons, New Jersey, USA, 2009), 10.1002/9780470686621.
- [69] CMS Collaboration, Measurement of prompt open-charm production cross sections in proton-proton collisions at $\sqrt{s} = 13$ TeV, *J. High Energy Phys.* **11** (2021) 225.
- [70] J. M. Blatt and V. F. Weisskopf, *Theoretical Nuclear Physics* (Springer, New York, 1952), 10.1007/978-1-4612-9959-2.
- [71] L. Lyons, D. Gibaut, and P. Clifford, How to combine correlated estimates of a single physical quantity, *Nucl. Instrum. Methods Phys. Res., Sect. A* **270**, 110 (1988).
- [72] R. Nisius, On the combination of correlated estimates of a physics observable, *Eur. Phys. J. C* **74**, 3004 (2014).
- [73] R. Nisius, BLUE: Combining correlated estimates of physics observables within ROOT using the best linear unbiased estimate method, *SoftwareX* **11**, 100468 (2020).

A. Hayrapetyan,¹ A. Tumasyan,^{1,b} W. Adam,² J. W. Andrejkovic,² T. Bergauer,² S. Chatterjee,² K. Damanakis,² M. Dragicevic,² P. S. Hussain,² M. Jeitler,^{2,c} N. Krammer,² A. Li,² D. Liko,² I. Mikulec,² J. Schieck,^{2,c} R. Schöfbeck,² D. Schwarz,² M. Sonawane,² S. Templ,² W. Waltenberger,² C.-E. Wulz,^{2,c} M. R. Darwish,^{3,d} T. Janssen,³ P. Van Mechelen,³ E. S. Bols,⁴ J. D'Hondt,⁴ S. Dansana,⁴ A. De Moor,⁴ M. Delcourt,⁴ S. Lowette,⁴ I. Makarenko,⁴ D. Müller,⁴ S. Tavernier,⁴ M. Tytgat,^{4,e} G. P. Van Onsem,⁴ S. Van Putte,⁴ D. Vannerom,⁴ B. Clerbaux,⁵ A. K. Das,⁵ G. De Lentdecker,⁵ H. Evard,⁵ L. Favart,⁵ P. Gianneios,⁵ D. Hohov,⁵ J. Jaramillo,⁵ A. Khalilzadeh,⁵ F. A. Khan,⁵ K. Lee,⁵ M. Mahdavikhorrami,⁵ A. Malara,⁵ S. Paredes,⁵ L. Thomas,⁵ M. Vanden Bemden,⁵ C. Vander Velde,⁵ P. Vanlaer,⁵ M. De Coen,⁶ D. Dobur,⁶ Y. Hong,⁶ J. Knolle,⁶ L. Lambrecht,⁶ G. Mestdach,⁶ K. Mota Amarilo,⁶ C. Rendón,⁶ A. Samalan,⁶ K. Skovpen,⁶ N. Van Den Bossche,⁶ J. van der Linden,⁶ L. Wezenbeek,⁶ A. Benecke,⁷ A. Bethani,⁷ G. Bruno,⁷ C. Caputo,⁷ C. Delaere,⁷ I. S. Donertas,⁷ A. Giannmanco,⁷ Sa. Jain,⁷ V. Lemaitre,⁷ J. Lidrych,⁷ P. Mastrapasqua,⁷ T. T. Tran,⁷ S. Wertz,⁷ G. A. Alves,⁸ E. Coelho,⁸ C. Hensel,⁸ T. Menezes De Oliveira,⁸ A. Moraes,⁸ P. Rebello Teles,⁸ M. Soeiro,⁸ W. L. Aldá Júnior,⁹ M. Alves Gallo Pereira,⁹ M. Barroso Ferreira Filho,⁹ H. Brandao Malbouisson,⁹ W. Carvalho,⁹ J. Chinellato,^{9,f} E. M. Da Costa,⁹ G. G. Da Silveira,^{9,g} D. De Jesus Damiao,⁹ S. Fonseca De Souza,⁹ R. Gomes De Souza,⁹ M. Macedo,⁹ J. Martins,^{9,h} C. Mora Herrera,⁹ L. Mundim,⁹ H. Nogima,⁹ J. P. Pinheiro,⁹ A. Santoro,⁹ A. Sznajder,⁹ M. Thiel,⁹ A. Vilela Pereira,⁹ C. A. Bernardes,^{10,g} L. Calligaris,¹⁰ T. R. Fernandez Perez Tomei,¹⁰ E. M. Gregores,¹⁰ P. G. Mercadante,¹⁰ S. F. Novaes,¹⁰ B. Orzari,¹⁰ Sandra S. Padula,¹⁰ A. Aleksandrov,¹¹ G. Antchev,¹¹ R. Hadjiiska,¹¹ P. Iaydjiev,¹¹ M. Misheva,¹¹ M. Shopova,¹¹ G. Sultanov,¹¹ A. Dimitrov,¹² L. Litov,¹² B. Pavlov,¹² P. Petkov,¹² A. Petrov,¹² E. Shumka,¹² S. Keshri,¹³ S. Thakur,¹³ T. Cheng,¹⁴ T. Javaid,¹⁴ L. Yuan,¹⁴ Z. Hu,¹⁵ J. Liu,¹⁵ K. Yi,^{15,i,j} G. M. Chen,^{16,k}

- H. S. Chen^{16,k}, M. Chen^{16,k}, F. Iemmi¹⁶, C. H. Jiang¹⁶, A. Kapoor^{16,l}, H. Liao¹⁶, Z.-A. Liu^{16,m}, R. Sharma^{16,n}, J. N. Song^{16,m}, J. Tao¹⁶, C. Wang^{16,k}, J. Wang¹⁶, Z. Wang^{16,k}, H. Zhang¹⁶, A. Agapitos¹⁷, Y. Ban¹⁷, A. Levin¹⁷, C. Li¹⁷, Q. Li¹⁷, Y. Mao¹⁷, S. J. Qian¹⁷, X. Sun¹⁷, D. Wang¹⁷, H. Yang¹⁷, L. Zhang¹⁷, C. Zhou¹⁷, Z. You¹⁸, K. Jaffel¹⁹, N. Lu¹⁹, G. Bauer^{20,o}, X. Gao^{21,p}, Z. Lin²², C. Lu²², M. Xiao²², C. Avila²³, D. A. Barbosa Trujillo, A. Cabrera²³, C. Florez²³, J. Fraga²³, J. A. Reyes Vega²³, J. Mejia Guisao²⁴, F. Ramirez²⁴, M. Rodriguez²⁴, J. D. Ruiz Alvarez²⁴, D. Giljanovic²⁵, N. Godinovic²⁵, D. Lelas²⁵, A. Sculac²⁵, M. Kovac²⁶, T. Sculac²⁶, P. Bargassa²⁷, V. Brigljevic²⁷, B. K. Chitroda²⁷, D. Ferencek²⁷, K. Jakovcic²⁷, S. Mishra²⁷, A. Starodumov^{27,q}, T. Susa²⁷, A. Attikis²⁸, K. Christoforou²⁸, A. Hadjigapiou²⁸, S. Konstantinou²⁸, J. Mousa²⁸, C. Nicolaou²⁸, L. Paizanos²⁸, F. Ptochos²⁸, P. A. Razis²⁸, H. Rykaczewski²⁸, H. Saka²⁸, A. Stepennov²⁸, M. Finger²⁹, M. Finger Jr.²⁹, A. Kveton²⁹, E. Ayala³⁰, E. Carrera Jarrin³¹, Y. Assran,^{32,r,s} S. Elgammal,^{32,s} M. A. Mahmoud³³, Y. Mohammed³³, K. Ehataht³⁴, M. Kadastik,³⁴ T. Lange³⁴, S. Nandan³⁴, C. Nielsen³⁴, J. Pata³⁴, M. Raidal³⁴, L. Tani³⁴, C. Veelken³⁴, H. Kirschenmann³⁵, K. Osterberg³⁵, M. Voutilainen³⁵, S. Bharthuar³⁶, E. Brücken³⁶, F. Garcia³⁶, K. T. S. Kallonen³⁶, R. Kinnunen³⁶, T. Lampén³⁶, K. Lassila-Perini³⁶, S. Lehti³⁶, T. Lindén³⁶, L. Martikainen³⁶, M. Myllymäki³⁶, M. m. Rantanen³⁶, H. Siikonen³⁶, E. Tuominen³⁶, J. Tuominenemi³⁶, P. Luukka³⁷, H. Petrow³⁷, M. Besancon³⁸, F. Couderc³⁸, M. Dejardin³⁸, D. Denegri,³⁸ J. L. Faure,³⁸ F. Ferri³⁸, S. Ganjour³⁸, P. Gras³⁸, G. Hamel de Monchenault³⁸, V. Lohezic³⁸, J. Malcles³⁸, F. Orlandi³⁸, L. Portales³⁸, J. Rander,³⁸ A. Rosowsky³⁸, M. Ö. Sahin³⁸, A. Savoy-Navarro^{38,t}, P. Simkina³⁸, M. Titov³⁸, M. Tornago³⁸, F. Beaudette³⁹, A. Buchot Perraguin³⁹, P. Busson³⁹, A. Cappati³⁹, C. Charlott³⁹, M. Chiusi³⁹, F. Damas³⁹, O. Davignon³⁹, A. De Wit³⁹, I. T. Ehle³⁹, B. A. Fontana Santos Alves³⁹, S. Ghosh³⁹, A. Gilbert³⁹, R. Granier de Cassagnac³⁹, A. Hakimi³⁹, B. Harikrishnan³⁹, L. Kalipoliti³⁹, G. Liu³⁹, J. Motta³⁹, M. Nguyen³⁹, C. Ochando³⁹, R. Salerno³⁹, J. B. Sauvan³⁹, Y. Sirois³⁹, A. Tarabini³⁹, E. Vernazza³⁹, A. Zabi³⁹, A. Zghiche³⁹, J.-L. Agram^{40,u}, J. Andrea⁴⁰, D. Apparù⁴⁰, D. Bloch⁴⁰, J.-M. Brom⁴⁰, E. C. Chabert⁴⁰, C. Collard⁴⁰, S. Falke⁴⁰, U. Goerlach⁴⁰, C. Grimault,⁴⁰ R. Haeberle⁴⁰, A.-C. Le Bihan⁴⁰, M. Meena⁴⁰, G. Saha⁴⁰, M. A. Sessini⁴⁰, P. Van Hove⁴⁰, S. Beauceron⁴¹, B. Blançon⁴¹, G. Boudoul⁴¹, N. Chanon⁴¹, D. Contardo⁴¹, P. Depasse⁴¹, C. Dozen^{41,v}, H. El Mamouni,⁴¹ J. Fay⁴¹, S. Gascon⁴¹, M. Gouzevitch⁴¹, C. Greenberg,⁴¹ G. Grenier⁴¹, B. Ille⁴¹, I. B. Laktineh,⁴¹ M. Lethuillier⁴¹, L. Mirabito,⁴¹ S. Perries,⁴¹ A. Purohit⁴¹, M. Vander Donckt⁴¹, P. Verdier⁴¹, J. Xiao⁴¹, I. Lomidze⁴², T. Toriashvili^{42,w}, Z. Tsamalaidze^{42,q}, V. Botta⁴³, L. Feld⁴³, K. Klein⁴³, M. Lipinski⁴³, D. Meuser⁴³, A. Pauls⁴³, N. Röwert⁴³, M. Teroerde⁴³, S. Diekmann⁴⁴, A. Dodonova⁴⁴, N. Eich⁴⁴, D. Eliseev⁴⁴, F. Engelke⁴⁴, J. Erdmann,⁴⁴ M. Erdmann⁴⁴, P. Fackeldey⁴⁴, B. Fischer⁴⁴, T. Hebbeker⁴⁴, K. Hoepfner⁴⁴, F. Ivone⁴⁴, A. Jung⁴⁴, M. y. Lee⁴⁴, F. Mausolf⁴⁴, M. Merschmeyer⁴⁴, A. Meyer⁴⁴, S. Mukherjee⁴⁴, D. Noll⁴⁴, F. Nowotny,⁴⁴ A. Pozdnyakov⁴⁴, Y. Rath,⁴⁴ W. Redjeb⁴⁴, F. Rehm,⁴⁴ H. Reithler⁴⁴, U. Sarkar⁴⁴, V. Sarkisovi⁴⁴, A. Schmidt⁴⁴, A. Sharma⁴⁴, J. L. Spah⁴⁴, A. Stein⁴⁴, F. Torres Da Silva De Araujo^{44,x}, S. Wiedenbeck⁴⁴, S. Zaleski,⁴⁴ C. Dziwok⁴⁵, G. Flügge⁴⁵, W. Haj Ahmad^{45,y}, T. Kress⁴⁵, A. Nowack⁴⁵, O. Pooth⁴⁵, A. Stahl⁴⁵, T. Ziemons⁴⁵, A. Zott⁴⁵, H. Aarup Petersen⁴⁶, M. Aldaya Martin⁴⁶, J. Alimena⁴⁶, S. Amoroso,⁴⁶ Y. An⁴⁶, S. Baxter⁴⁶, M. Bayatmakou⁴⁶, H. Becerril Gonzalez⁴⁶, O. Behnke⁴⁶, A. Belvedere⁴⁶, S. Bhattacharya⁴⁶, F. Blekman^{46,z}, K. Borras^{46,aa}, A. Campbell⁴⁶, A. Cardini⁴⁶, C. Cheng⁴⁶, F. Colombina⁴⁶, S. Consuegra Rodríguez⁴⁶, G. Correia Silva⁴⁶, M. De Silva⁴⁶, G. Eckerlin,⁴⁶ D. Eckstein⁴⁶, L. I. Estevez Banos⁴⁶, O. Filatov⁴⁶, E. Gallo^{46,z}, A. Geiser⁴⁶, A. Giraldi⁴⁶, V. Guglielmi⁴⁶, M. Guthoff⁴⁶, A. Hinzmann⁴⁶, A. Jafari^{46,bb}, L. Jeppe⁴⁶, B. Kaech⁴⁶, M. Kasemann⁴⁶, C. Kleinwort⁴⁶, R. Kogler⁴⁶, M. Komm⁴⁶, D. Krücker⁴⁶, W. Lange⁴⁶, D. Leyva Pernia⁴⁶, K. Lipka^{46,cc}, W. Lohmann^{46,dd}, F. Lorkowski⁴⁶, R. Mankel⁴⁶, I.-A. Melzer-Pellmann⁴⁶, M. Mendizabal Morentin⁴⁶, A. B. Meyer⁴⁶, G. Milella⁴⁶, A. Mussgiller⁴⁶, L. P. Nair⁴⁶, A. Nürnberg⁴⁶, Y. Otarid⁴⁶, J. Park⁴⁶, D. Pérez Adán⁴⁶, E. Ranken⁴⁶, A. Raspereza⁴⁶, D. Rastorguev⁴⁶, B. Ribeiro Lopes⁴⁶, J. Rübenach,⁴⁶ A. Saggio⁴⁶, M. Scham^{46,ee,aa}, S. Schnake^{46,aa}, P. Schütze⁴⁶, C. Schwanenberger^{46,z}, D. Selivanova⁴⁶, K. Sharko⁴⁶, M. Shchedrolosiev⁴⁶, R. E. Sosa Ricardo⁴⁶, D. Stafford,⁴⁶ F. Vazzoler⁴⁶, A. Ventura Barroso⁴⁶, R. Walsh⁴⁶, Q. Wang⁴⁶, Y. Wen⁴⁶, K. Wichmann,⁴⁶ L. Wiens^{46,aa}, C. Wissing⁴⁶, Y. Yang⁴⁶, A. Zimmermann Castro Santos⁴⁶, A. Albrecht⁴⁷, S. Albrecht⁴⁷, M. Antonello⁴⁷, S. Bein⁴⁷, L. Benato⁴⁷, S. Bollweg⁴⁷, M. Bonanomi⁴⁷, P. Connor⁴⁷, K. El Morabit⁴⁷, Y. Fischer⁴⁷, E. Garutti⁴⁷, A. Grohsjean⁴⁷, J. Haller⁴⁷, H. R. Jabusch⁴⁷, G. Kasieczka⁴⁷, P. Keicher,⁴⁷ R. Klanner⁴⁷, W. Korcari⁴⁷, T. Kramer⁴⁷, V. Kutzner⁴⁷, F. Labe⁴⁷, J. Lange⁴⁷, A. Lobanov⁴⁷, C. Matthies⁴⁷, L. Moureaux⁴⁷, M. Mrowietz,⁴⁷

- A. Nigamova⁴⁷ Y. Nissan⁴⁷ A. Paasch⁴⁷ K. J. Pena Rodriguez⁴⁷ T. Quadfasel⁴⁷ B. Raciti⁴⁷ M. Rieger⁴⁷
 D. Savoio⁴⁷ J. Schindler⁴⁷ P. Schleper⁴⁷ M. Schröder⁴⁷ J. Schwandt⁴⁷ M. Sommerhalder⁴⁷ H. Stadie⁴⁷
 G. Steinbrück⁴⁷ A. Tews⁴⁷ M. Wolf⁴⁷ S. Brommer⁴⁸ M. Burkart⁴⁸ E. Butz⁴⁸ T. Chwalek⁴⁸ A. Dierlamm⁴⁸
 A. Droll⁴⁸ N. Faltermann⁴⁸ M. Giffels⁴⁸ A. Gottmann⁴⁸ F. Hartmann^{48,ff} R. Hofsaess⁴⁸ M. Horzela⁴⁸
 U. Husemann⁴⁸ J. Kieseler⁴⁸ M. Klute⁴⁸ R. Koppenhöfer⁴⁸ J. M. Lawhorn⁴⁸ M. Link⁴⁸ A. Lintuluoto⁴⁸
 B. Maier⁴⁸ S. Maier⁴⁸ S. Mitra⁴⁸ M. Mormile⁴⁸ Th. Müller⁴⁸ M. Neukum⁴⁸ M. Oh⁴⁸ E. Pfeffer⁴⁸
 M. Presilla⁴⁸ G. Quast⁴⁸ K. Rabbertz⁴⁸ B. Regnery⁴⁸ N. Shadskiy⁴⁸ I. Shvetsov⁴⁸ H. J. Simonis⁴⁸
 M. Toms⁴⁸ N. Trevisani⁴⁸ R. F. Von Cube⁴⁸ M. Wassmer⁴⁸ S. Wieland⁴⁸ F. Wittig⁴⁸ R. Wolf⁴⁸ X. Zuo⁴⁸
 G. Anagnostou⁴⁹ G. Daskalakis⁴⁹ A. Kyriakis⁴⁹ A. Papadopoulos^{49,ff} A. Stakia⁴⁹ P. Kontaxakis⁴⁹
 G. Melachroinos⁵⁰ Z. Painesis⁵⁰ A. Panagiotou⁵⁰ I. Papavergou⁵⁰ I. Paraskevas⁵⁰ N. Saoulidou⁵⁰
 K. Theofilatos⁵⁰ E. Tziaferi⁵⁰ K. Vellidis⁵⁰ I. Zisopoulos⁵⁰ G. Bakas⁵¹ T. Chatzistavrou⁵¹ G. Karapostoli⁵¹
 K. Kousouris⁵¹ I. Papakrivosopoulos⁵¹ E. Siamarkou⁵¹ G. Tsipolitis⁵¹ A. Zacharopoulou⁵¹ K. Adamidis⁵²
 I. Bestintzanos⁵² I. Evangelou⁵² C. Foudas⁵² C. Kamtsikis⁵² P. Katsoulis⁵² P. Kokkas⁵²
 P. G. Kosmoglou Kioseoglou⁵² N. Manthos⁵² I. Papadopoulos⁵² J. Strologas⁵² M. Bartók^{53,gg} C. Hajdu⁵³
 D. Horvath^{53,hh,ii} K. Márton⁵³ A. J. Rádl^{53,jj} F. Sikler⁵³ V. Veszpremi⁵³ M. Csanád⁵⁴ K. Farkas⁵⁴
 M. M. A. Gadallah^{54,kk} Á. Kadlecik⁵⁴ P. Major⁵⁴ K. Mandal⁵⁴ G. Pásztor⁵⁴ G. I. Veres⁵⁴ P. Raics⁵⁵
 B. Ujvari⁵⁵ G. Zilizi⁵⁵ G. Bencze⁵⁶ S. Czellar⁵⁶ J. Molnar⁵⁶ Z. Szillasi⁵⁶ T. Csorgo^{57,ll} F. Nemes^{57,ll} T. Novak⁵⁷
 J. Babbar⁵⁸ S. Bansal⁵⁸ S. B. Beri⁵⁸ V. Bhatnagar⁵⁸ G. Chaudhary⁵⁸ S. Chauhan⁵⁸ N. Dhingra^{58,mm}
 A. Kaur⁵⁸ A. Kaur⁵⁸ H. Kaur⁵⁸ M. Kaur⁵⁸ S. Kumar⁵⁸ K. Sandeep⁵⁸ T. Sheokand⁵⁸ J. B. Singh⁵⁸
 A. Singla⁵⁸ A. Ahmed⁵⁹ A. Bhardwaj⁵⁹ A. Chhetri⁵⁹ B. C. Choudhary⁵⁹ A. Kumar⁵⁹ A. Kumar⁵⁹
 M. Naimuddin⁵⁹ K. Ranjan⁵⁹ S. Saumya⁵⁹ S. Baradia⁶⁰ S. Barman^{60,nn} S. Bhattacharya⁶⁰ S. Dutta⁶⁰
 S. Dutta⁶⁰ S. Sarkar⁶⁰ M. M. Ameen⁶¹ P. K. Behera⁶¹ S. C. Behera⁶¹ S. Chatterjee⁶¹ P. Jana⁶¹ P. Kalbhor⁶¹
 J. R. Komaragiri^{61,oo} D. Kumar^{61,oo} P. R. Pujahari⁶¹ N. R. Saha⁶¹ A. Sharma⁶¹ A. K. Sikdar⁶¹ S. Verma⁶¹
 S. Dugad⁶² M. Kumar⁶² G. B. Mohanty⁶² P. Suryadevara⁶² A. Bala⁶³ S. Banerjee⁶³ R. M. Chatterjee⁶³
 R. K. Dewanjee^{63,pp} M. Guchait⁶³ Sh. Jain⁶³ A. Jaiswal⁶³ S. Kumar⁶³ G. Majumder⁶³ K. Mazumdar⁶³
 S. Parolia⁶³ A. Thachayath⁶³ S. Bahinipati^{64,qq} C. Kar⁶⁴ D. Maity^{64,rr} P. Mal⁶⁴ T. Mishra⁶⁴
 V. K. Muraleedharan Nair Bindhu^{64,rr} K. Naskar^{64,rr} A. Nayak^{64,rr} P. Sadangi⁶⁴ S. K. Swain⁶⁴ S. Varghese^{64,rr}
 D. Vats^{64,rr} S. Acharya^{65,ss} A. Alpana⁶⁵ S. Dube⁶⁵ B. Gomber^{65,ss} P. Hazarika⁶⁵ B. Kansal⁶⁵ A. Laha⁶⁵
 B. Sahu^{65,ss} S. Sharma⁶⁵ K. Y. Vaish⁶⁵ H. Bakhshiansohi^{66,tt} E. Khazaie^{66,uu} M. Zeinali^{66,vv} S. Bashiri⁶⁷
 S. Chenarani^{67,ww} S. M. Etesami⁶⁷ M. Khakzad⁶⁷ M. Mohammadi Najafabadi⁶⁷ S. Tizchang⁶⁷
 M. Grunewald⁶⁸ M. Abbrescia^{69a,69b} R. Aly^{69a,69c,xx} A. Colaleo^{69a,69b} D. Creanza^{69a,69c} B. D'Anzi^{69a,69b}
 N. De Filippis^{69a,69c} M. De Palma^{69a,69b} A. Di Florio^{69a,69c} W. Elmetenawee^{69a,69b,xx} L. Fiore^{69a} G. Iaselli^{69a,69c}
 M. Louka^{69a,69b} G. Maggi^{69a,69c} M. Maggi^{69a} I. Margjeka^{69a,69b} V. Mastrapasqua^{69a,69b} S. My^{69a,69b}
 S. Nuzzo^{69a,69b} A. Pellecchia^{69a,69b} A. Pompili^{69a,69b} G. Pugliese^{69a,69c} R. Radogna^{69a}
 G. Ramirez-Sanchez^{69a,69c} D. Ramos^{69a} A. Ranieri^{69a} L. Silvestris^{69a} F. M. Simone^{69a,69b} Ü. Sözbilir^{69a}
 A. Stamerra^{69a} R. Venditti^{69a} P. Verwilligen^{69a} A. Zaza^{69a,69b} G. Abbiendi^{70a} C. Battilana^{70a,70b}
 D. Bonacorsi^{70a,70b} L. Borgonovi^{70a} P. Capiluppi^{70a,70b} A. Castro^{70a,70b} F. R. Cavallo^{70a} M. Cuffiani^{70a,70b}
 G. M. Dallavalle^{70a} T. Diotalevi^{70a,70b} F. Fabbri^{70a} A. Fanfani^{70a,70b} D. Fasanella^{70a,70b} P. Giacomelli^{70a}
 L. Giommi^{70a,70b} C. Grandi^{70a} L. Guiducci^{70a,70b} S. Lo Meo^{70a,yy} L. Lunerti^{70a,70b} S. Marcellini^{70a}
 G. Masetti^{70a} F. L. Navarria^{70a,70b} A. Perrotta^{70a} F. Primavera^{70a,70b} A. M. Rossi^{70a,70b} T. Rovelli^{70a,70b}
 G. P. Siroli^{70a,70b} S. Costa^{71a,71b,zz} A. Di Mattia^{71a} R. Potenza^{71a,71b} A. Tricomi^{71a,71b,zz} C. Tuve^{71a,71b}
 P. Assiouras^{72a} G. Barbagli^{72a} G. Bardelli^{72a,72b} B. Camaiani^{72a,72b} A. Cassese^{72a} R. Ceccarelli^{72a}
 V. Ciulli^{72a,72b} C. Civinini^{72a} R. D'Alessandro^{72a,72b} E. Focardi^{72a,72b} T. Kello^{72a} G. Latino^{72a,72b} P. Lenzi^{72a,72b}
 M. Lizzo^{72a} M. Meschini^{72a} S. Paoletti^{72a} A. Papanastassiou^{72a,72b} G. Sguazzoni^{72a} L. Viliani^{72a} L. Benussi⁷³
 S. Bianco⁷³ S. Meola^{73,aaa} D. Piccolo⁷³ P. Chatagnon^{74a} F. Ferro^{74a} E. Robutti^{74a} S. Tosi^{74a,74b}
 A. Benaglia^{75a} G. Boldrini^{75a,75b} F. Brivio^{75a} F. Cetorelli^{75a} F. De Guio^{75a,75b} M. E. Dinardo^{75a,75b} P. Dini^{75a}
 S. Gennai^{75a} R. Gerosa^{75a,75b} A. Ghezzi^{75a,75b} P. Govoni^{75a,75b} L. Guzzi^{75a} M. T. Lucchini^{75a,75b}
 M. Malberti^{75a} S. Malvezzi^{75a} A. Massironi^{75a} D. Menasce^{75a} L. Moroni^{75a} M. Paganoni^{75a,75b}
 S. Palluotto^{75a,75b} D. Pedrini^{75a} B. S. Pinolini^{75a} G. Pizzati^{75a,75b} S. Ragazzi^{75a,75b} T. Tabarelli de Fatis^{75a,75b}

- S. Buontempo^{76a}, A. Cagnotta^{76a,76b}, F. Carnevali,^{76a,76b} N. Cavallo^{76a,76c}, F. Fabozzi^{76a,76c}, A. O. M. Iorio^{76a,76b}, L. Lista^{76a,76b,bbb}, P. Paolucci^{76a,ff}, B. Rossi^{76a}, C. Sciacca^{76a,76b}, R. Ardino^{77a}, P. Azzi^{77a}, N. Bacchetta^{77a,ccc}, A. Bergnoli^{77a}, D. Bisello^{77a,77b}, P. Bortignon^{77a}, G. Bortolato,^{77a,77b} A. Bragagnolo^{77a,77b}, A. C. M. Bulla^{77a}, R. Carlin^{77a,77b}, P. Checchia^{77a}, T. Dorigo^{77a}, F. Gasparini^{77a,77b}, U. Gasparini^{77a,77b}, E. Lusiani^{77a}, M. Margoni^{77a,77b}, F. Marini^{77a}, A. T. Meneguzzo^{77a,77b}, M. Migliorini^{77a,77b}, J. Pazzini^{77a,77b}, P. Ronchese^{77a,77b}, R. Rossin^{77a,77b}, F. Simonetto^{77a,77b}, G. Strong^{77a}, M. Tosi^{77a,77b}, A. Triossi^{77a,77b}, M. Zanetti^{77a,77b}, P. Zotto^{77a,77b}, A. Zucchetta^{77a,77b}, G. Zumerle^{77a,77b}, S. Abu Zeid^{78a,ddd}, C. Aimè^{78a,78b}, A. Braghieri^{78a}, S. Calzaferri^{78a}, D. Fiorina^{78a}, P. Montagna^{78a,78b}, V. Re^{78a}, C. Riccardi^{78a,78b}, P. Salvini^{78a}, I. Vai^{78a,78b}, P. Vitulo^{78a,78b}, S. Ajmal^{79a,79b}, G. M. Bilei^{79a}, D. Ciangottini^{79a,79b}, L. Fanò^{79a,79b}, M. Magherini^{79a,79b}, V. Mariani^{79a,79b}, M. Menichelli^{79a}, F. Moscatelli^{79a,eee}, A. Rossi^{79a,79b}, A. Santocchia^{79a,79b}, D. Spiga^{79a}, T. Tedeschi^{79a,79b}, P. Asenov^{80a,80b}, P. Azzurri^{80a}, G. Bagliesi^{80a}, R. Bhattacharya^{80a}, L. Bianchini^{80a,80b}, T. Boccali^{80a}, E. Bossini^{80a}, D. Bruschini^{80a,80c}, R. Castaldi^{80a}, M. A. Ciocci^{80a,80b}, M. Cipriani^{80a,80b}, V. D'Amante^{80a,80d}, R. Dell'Orso^{80a}, S. Donato^{80a}, A. Giassi^{80a}, F. Ligabue^{80a,80c}, D. Matos Figueiredo^{80a}, A. Messineo^{80a,80b}, M. Musich^{80a,80b}, F. Palla^{80a}, A. Rizzi^{80a,80b}, G. Rolandi^{80a,80c}, S. Roy Chowdhury^{80a}, T. Sarkar^{80a}, A. Scribano^{80a}, P. Spagnolo^{80a}, R. Tenchini^{80a}, G. Tonelli^{80a,80b}, N. Turini^{80a,80d}, F. Vaselli^{80a,80c}, A. Venturi^{80a}, P. G. Verdini^{80a}, C. Baldenegro Barrera^{81a,81b}, P. Barria^{81a}, C. Basile^{81a,81b}, M. Campana^{81a,81b}, F. Cavallari^{81a}, L. Cunqueiro Mendez^{81a,81b}, D. Del Re^{81a,81b}, E. Di Marco^{81a}, M. Diemoz^{81a}, F. Errico^{81a,81b}, E. Longo^{81a,81b}, P. Meridiani^{81a}, J. Mijuskovic^{81a,81b}, G. Organtini^{81a,81b}, F. Pandolfi^{81a}, R. Paramatti^{81a,81b}, C. Quaranta^{81a,81b}, S. Rahatlou^{81a,81b}, C. Rovelli^{81a}, F. Santanastasio^{81a,81b}, L. Soffi^{81a}, N. Amapane^{82a,82b}, R. Arcidiacono^{82a,82c}, S. Argiro^{82a,82b}, M. Arneodo^{82a,82c}, N. Bartosik^{82a}, R. Bellan^{82a,82b}, A. Bellora^{82a,82b}, C. Biino^{82a}, C. Borca^{82a,82b}, N. Cartiglia^{82a}, M. Costa^{82a,82b}, R. Covarelli^{82a,82b}, N. Demaria^{82a}, L. Finco^{82a}, M. Grippo^{82a,82b}, B. Kiani^{82a,82b}, F. Legger^{82a}, F. Luongo^{82a,82b}, C. Mariotti^{82a}, L. Markovic^{82a,82b}, S. Maselli^{82a}, A. Mecca^{82a,82b}, E. Migliore^{82a,82b}, M. Monteno^{82a}, R. Mulargia^{82a}, M. M. Obertino^{82a,82b}, G. Ortona^{82a}, L. Pacher^{82a,82b}, N. Pastrone^{82a}, M. Pelliccioni^{82a}, M. Ruspa^{82a,82c}, F. Siviero^{82a,82b}, V. Sola^{82a,82b}, A. Solano^{82a,82b}, A. Staiano^{82a}, C. Tarricone^{82a,82b}, D. Trocino^{82a}, G. Umoret^{82a,82b}, E. Vlasov^{82a,82b}, R. White^{82a}, S. Belforte^{83a}, V. Candelise^{83a,83b}, M. Casarsa^{83a}, F. Cossutti^{83a}, K. De Leo^{83a}, G. Della Ricca^{83a,83b}, S. Dogra⁸⁴, J. Hong⁸⁴, C. Huh⁸⁴, B. Kim⁸⁴, D. H. Kim⁸⁴, J. Kim⁸⁴, H. Lee⁸⁴, S. W. Lee⁸⁴, C. S. Moon⁸⁴, Y. D. Oh⁸⁴, M. S. Ryu⁸⁴, S. Sekmen⁸⁴, Y. C. Yang⁸⁴, M. S. Kim⁸⁵, G. Bak⁸⁶, P. Gwak⁸⁶, H. Kim⁸⁶, D. H. Moon⁸⁶, E. Asilar⁸⁷, J. Choi⁸⁷, D. Kim⁸⁷, T. J. Kim⁸⁷, J. A. Merlin⁸⁷, S. Choi⁸⁸, S. Han⁸⁸, B. Hong⁸⁸, K. Lee⁸⁸, K. S. Lee⁸⁸, S. Lee⁸⁸, J. Park⁸⁸, S. K. Park⁸⁸, J. Yoo⁸⁸, J. Goh⁸⁹, S. Yang⁸⁹, H. S. Kim⁹⁰, Y. Kim⁹⁰, S. Lee⁹⁰, J. Almond⁹¹, J. H. Bhyun⁹¹, J. Choi⁹¹, W. Jun⁹¹, J. Kim⁹¹, S. Ko⁹¹, H. Kwon⁹¹, H. Lee⁹¹, J. Lee⁹¹, J. Lee⁹¹, B. H. Oh⁹¹, S. B. Oh⁹¹, H. Seo⁹¹, U. K. Yang⁹¹, I. Yoon⁹¹, W. Jang⁹², D. Y. Kang⁹², Y. Kang⁹², S. Kim⁹², B. Ko⁹², J. S. H. Lee⁹², Y. Lee⁹², I. C. Park⁹², Y. Roh⁹², I. J. Watson⁹², S. Ha⁹³, H. D. Yoo⁹³, M. Choi⁹⁴, M. R. Kim⁹⁴, H. Lee⁹⁴, Y. Lee⁹⁴, I. Yu⁹⁵, T. Beyrouthy⁹⁵, K. Dreimanis⁹⁶, A. Gaile⁹⁶, G. Pikurs⁹⁶, A. Potrebko⁹⁶, M. Seidel⁹⁶, N. R. Strautnieks⁹⁷, M. Ambrozias⁹⁸, A. Juodagalvis⁹⁸, A. Rinkevicius⁹⁸, G. Tamulaitis⁹⁸, N. Bin Norjoharuddeen⁹⁹, I. Yusuff^{99,fff}, Z. Zolkapli⁹⁹, J. F. Benitez¹⁰⁰, A. Castaneda Hernandez¹⁰⁰, H. A. Encinas Acosta¹⁰⁰, L. G. Gallegos Marínez¹⁰⁰, M. León Coello¹⁰⁰, J. A. Murillo Quijada¹⁰⁰, A. Sehrawat¹⁰⁰, L. Valencia Palomo¹⁰⁰, G. Ayala¹⁰¹, H. Castilla-Valdez¹⁰¹, H. Crotte Ledesma¹⁰¹, E. De La Cruz-Burelo¹⁰¹, I. Heredia-De La Cruz^{101,ggg}, R. Lopez-Fernandez¹⁰¹, C. A. Mondragon Herrera¹⁰¹, A. Sánchez Hernández¹⁰¹, C. Oropeza Barrera¹⁰², M. Ramírez García¹⁰², I. Bautista¹⁰³, I. Pedraza¹⁰³, H. A. Salazar Ibarguen¹⁰³, C. Uribe Estrada¹⁰³, I. Bubanja¹⁰⁴, N. Raicevic¹⁰⁴, P. H. Butler¹⁰⁵, A. Ahmad¹⁰⁶, M. I. Asghar¹⁰⁶, A. Awais¹⁰⁶, M. I. M. Awan¹⁰⁶, H. R. Hoorani¹⁰⁶, W. A. Khan¹⁰⁶, V. Avati¹⁰⁷, L. Grzanka¹⁰⁷, M. Malawski¹⁰⁷, H. Bialkowska¹⁰⁸, M. Bluj¹⁰⁸, B. Boimska¹⁰⁸, M. Górski¹⁰⁸, M. Kazana¹⁰⁸, M. Szleper¹⁰⁸, P. Zalewski¹⁰⁸, K. Bunkowski¹⁰⁹, K. Doroba¹⁰⁹, A. Kalinowski¹⁰⁹, M. Konecki¹⁰⁹, J. Krolikowski¹⁰⁹, A. Muhammad¹⁰⁹, K. Pozniak¹¹⁰, W. Zabolotny¹¹⁰, M. Araujo¹¹¹, D. Bastos¹¹¹, C. Beirão Da Cruz E Silva¹¹¹, A. Boletti¹¹¹, M. Bozzo¹¹¹, T. Camporesi¹¹¹, G. Da Molin¹¹¹, P. Faccioli¹¹¹, M. Gallinaro¹¹¹, J. Hollar¹¹¹, N. Leonardo¹¹¹, T. Niknejad¹¹¹, A. Petrilli¹¹¹, M. Pisano¹¹¹, J. Seixas¹¹¹, J. Varela¹¹¹, J. W. Wulff¹¹¹, P. Adzic¹¹², P. Milenovic¹¹², M. Dordevic¹¹³, J. Milosevic¹¹³, V. Rekovic¹¹³, M. Aguilar-Benitez¹¹⁴, J. Alcaraz Maestre¹¹⁴, Cristina F. Bedoya¹¹⁴, Oliver M. Carretero¹¹⁴, M. Cepeda¹¹⁴, M. Cerrada¹¹⁴, N. Colino¹¹⁴, B. De La Cruz¹¹⁴, A. Delgado Peris¹¹⁴

- A. Escalante Del Valle¹¹⁴ D. Fernández Del Val¹¹⁴ J. P. Fernández Ramos¹¹⁴ J. Flix¹¹⁴ M. C. Fouz¹¹⁴
 O. Gonzalez Lopez¹¹⁴ S. Goy Lopez¹¹⁴ J. M. Hernandez¹¹⁴ M. I. Josa¹¹⁴ D. Moran¹¹⁴ C. M. Morcillo Perez¹¹⁴
 Á. Navarro Tobar¹¹⁴ C. Perez Dengra¹¹⁴ A. Pérez-Calero Yzquierdo¹¹⁴ J. Puerta Pelayo¹¹⁴ I. Redondo¹¹⁴
 D. D. Redondo Ferrero¹¹⁴ L. Romero¹¹⁴ S. Sánchez Navas¹¹⁴ L. Urda Gómez¹¹⁴ J. Vazquez Escobar¹¹⁴
 C. Willmott¹¹⁴ J. F. de Trocóniz¹¹⁵ B. Alvarez Gonzalez¹¹⁶ J. Cuevas¹¹⁶ J. Fernandez Menendez¹¹⁶
 S. Folgueras¹¹⁶ I. Gonzalez Caballero¹¹⁶ J. R. González Fernández¹¹⁶ P. Leguina¹¹⁶ E. Palencia Cortezon¹¹⁶
 C. Ramón Álvarez¹¹⁶ V. Rodríguez Bouza¹¹⁶ A. Soto Rodríguez¹¹⁶ A. Trapote¹¹⁶ C. Vico Villalba¹¹⁶
 P. Vischia¹¹⁶ S. Bhowmik¹¹⁷ S. Blanco Fernández¹¹⁷ J. A. Brochero Cifuentes¹¹⁷ I. J. Cabrillo¹¹⁷
 A. Calderon¹¹⁷ J. Duarte Campderros¹¹⁷ M. Fernandez¹¹⁷ G. Gomez¹¹⁷ C. Lasosa García¹¹⁷
 R. Lopez Ruiz¹¹⁷ C. Martinez Rivero¹¹⁷ P. Martinez Ruiz del Arbol¹¹⁷ F. Matorras¹¹⁷ P. Matorras Cuevas¹¹⁷
 E. Navarrete Ramos¹¹⁷ J. Piedra Gomez¹¹⁷ L. Scodellaro¹¹⁷ I. Vila¹¹⁷ J. M. Vizan Garcia¹¹⁷
 M. K. Jayananda¹¹⁸ B. Kailasapathy^{118,hhh} D. U. J. Sonnadar¹¹⁸ D. D. C. Wickramarathna¹¹⁸
 W. G. D. Dharmaratna^{119,iii} K. Liyanage¹¹⁹ N. Perera¹¹⁹ N. Wickramage¹¹⁹ D. Abbaneo¹²⁰ C. Amendola¹²⁰
 E. Auffray¹²⁰ G. Auzinger¹²⁰ J. Baechler¹²⁰ D. Barney¹²⁰ A. Bermúdez Martínez¹²⁰ M. Bianco¹²⁰ B. Bilin¹²⁰
 A. A. Bin Anuar¹²⁰ A. Bocci¹²⁰ C. Botta¹²⁰ E. Brondolin¹²⁰ C. Caiollo¹²⁰ G. Cerminara¹²⁰
 N. Chernyavskaya¹²⁰ D. d'Enterria¹²⁰ A. Dabrowski¹²⁰ A. David¹²⁰ A. De Roeck¹²⁰ M. M. Defranchis¹²⁰
 M. Deile¹²⁰ M. Dobson¹²⁰ L. Forthomme¹²⁰ G. Franzoni¹²⁰ W. Funk¹²⁰ S. Giani¹²⁰ D. Gigi¹²⁰ K. Gill¹²⁰
 F. Glege¹²⁰ L. Gouskos¹²⁰ M. Haranko¹²⁰ J. Hegeman¹²⁰ B. Huber¹²⁰ V. Innocente¹²⁰ T. James¹²⁰
 P. Janot¹²⁰ O. Kaluzinska¹²⁰ S. Laurila¹²⁰ P. Lecoq¹²⁰ E. Leutgeb¹²⁰ C. Lourenço¹²⁰ L. Malgeri¹²⁰
 M. Mannelli¹²⁰ A. C. Marini¹²⁰ M. Matthewman¹²⁰ A. Mehta¹²⁰ F. Meijers¹²⁰ S. Mersi¹²⁰ E. Meschi¹²⁰
 V. Milosevic¹²⁰ F. Monti¹²⁰ F. Moortgat¹²⁰ M. Mulders¹²⁰ I. Neutelings¹²⁰ S. Orfanelli¹²⁰ F. Pantaleo¹²⁰
 G. Petrucciani¹²⁰ A. Pfeiffer¹²⁰ M. Pierini¹²⁰ D. Piparo¹²⁰ H. Qu¹²⁰ D. Rabady¹²⁰ M. Rovere¹²⁰
 H. Sakulin¹²⁰ S. Scarfi¹²⁰ C. Schwick¹²⁰ M. Selvaggi¹²⁰ A. Sharma¹²⁰ K. Shchelina¹²⁰ P. Silva¹²⁰
 P. Sphicas^{120,iii} A. G. Stahl Leiton¹²⁰ A. Steen¹²⁰ S. Summers¹²⁰ D. Treille¹²⁰ P. Tropea¹²⁰ A. Tsirou¹²⁰
 D. Walter¹²⁰ J. Wanczyk^{120,kkk} J. Wang¹²⁰ S. Wuchterl¹²⁰ P. Zehetner¹²⁰ P. Zejdl¹²⁰ W. D. Zeuner¹²⁰
 T. Bevilacqua^{121,III} L. Caminada^{121,III} A. Ebrahimi¹²¹ W. Erdmann¹²¹ R. Horisberger¹²¹ Q. Ingram¹²¹
 H. C. Kaestli¹²¹ D. Kotlinski¹²¹ C. Lange¹²¹ M. Missiroli^{121,III} L. Noehte^{121,III} T. Rohe¹²¹ T. K. Arrestad¹²²
 K. Androsov¹²² M. Backhaus¹²² G. Bonomelli¹²² A. Calandri¹²² C. Cazzaniga¹²² K. Datta¹²²
 A. De Cosa¹²² G. Dissertori¹²² M. Dittmar¹²² M. Donegà¹²² F. Eble¹²² M. Galli¹²² K. Gedia¹²²
 F. Glessgen¹²² C. Grab¹²² N. Härringer¹²² T. G. Harte¹²² D. Hits¹²² W. Lustermann¹²² A.-M. Lyon¹²²
 R. A. Manzoni¹²² M. Marchegiani¹²² L. Marchese¹²² C. Martin Perez¹²² A. Mascellani^{122,kkk}
 F. Nessi-Tedaldi¹²² F. Pauss¹²² V. Perovic¹²² S. Pigazzini¹²² C. Reissel¹²² T. Reitenspiess¹²² B. Ristic¹²²
 F. Riti¹²² R. Seidita¹²² J. Steggemann^{122,kkk} D. Valsecchi¹²² R. Wallny¹²² C. Amsler^{123,mmm} P. Bärtschi¹²³
 M. F. Canelli¹²³ K. Cormier¹²³ J. K. Heikkilä¹²³ M. Huwiler¹²³ W. Jin¹²³ A. Jofrehei¹²³ B. Kilminster¹²³
 S. Leontsinis¹²³ S. P. Liechti¹²³ A. Macchiolo¹²³ P. Meiring¹²³ U. Molinatti¹²³ A. Reimers¹²³ P. Robmann¹²³
 S. Sanchez Cruz¹²³ M. Senger¹²³ E. Shokr¹²³ F. Stäger¹²³ Y. Takahashi¹²³ R. Tramontano¹²³ C. Adloff^{124,nnn}
 D. Bhowmik¹²⁴ C. M. Kuo¹²⁴ W. Lin¹²⁴ P. K. Rout¹²⁴ P. C. Tiwari^{124,ooo} S. S. Yu¹²⁴ L. Ceard¹²⁵ Y. Chao¹²⁵
 K. F. Chen¹²⁵ P. s. Chen¹²⁵ Z. g. Chen¹²⁵ A. De Iorio¹²⁵ W.-S. Hou¹²⁵ T. h. Hsu¹²⁵ Y. w. Kao¹²⁵ S. Karmakar¹²⁵
 R. Khurana¹²⁵ G. Kole¹²⁵ Y. y. Li¹²⁵ R.-S. Lu¹²⁵ E. Paganis¹²⁵ X. f. Su¹²⁵ J. Thomas-Wilsker¹²⁵ L. s. Tsai¹²⁵
 H. y. Wu¹²⁵ E. Yazgan¹²⁵ C. Asawatangtrakuldee¹²⁶ N. Srimanobhas¹²⁶ V. Wachirapusanand¹²⁶ D. Agyel¹²⁷
 F. Boran¹²⁷ Z. S. Demiroglu¹²⁷ F. Dolek¹²⁷ I. Dumanoglu^{127,ooo} E. Eskut¹²⁷ Y. Guler^{127,ppp}
 E. Gurpinar Guler^{127,ppp} C. Isik¹²⁷ O. Kara¹²⁷ A. Kayis Topaksu¹²⁷ U. Kiminsu¹²⁷ G. Onengut¹²⁷
 K. Ozdemir^{127,qqq} A. Polatoz¹²⁷ B. Tali^{127,rrr} U. G. Tok¹²⁷ S. Turkcapar¹²⁷ E. Uslan¹²⁷ I. S. Zorbakir¹²⁷
 G. Sokmen¹²⁸ M. Yalvac^{128,sss} B. Akgun¹²⁹ I. O. Atakisi¹²⁹ E. Gülmez¹²⁹ M. Kaya^{129,ttt} O. Kaya^{129,uuu}
 S. Tekten^{129,vvv} A. Cakir¹³⁰ K. Cankocak^{130,ooo,www} G. G. Dincer¹³⁰ Y. Komurcu¹³⁰ S. Sen^{130,xxx}
 O. Aydilek^{131,y} S. Cerci^{131,rrr} V. Epshteyn¹³¹ B. Hacisahinoglu¹³¹ I. Hos^{131,yyy} B. Kaynak¹³¹
 S. Ozkorucuklu¹³¹ O. Potok¹³¹ H. Sert¹³¹ C. Simsek¹³¹ C. Zorbilmez¹³¹ B. Isildak^{132,zzz} D. Sunar Cerci^{132,rrr}
 A. Boyaryntsev¹³³ B. Grynyov¹³³ L. Levchuk¹³⁴ D. Anthony¹³⁵ J. J. Brooke¹³⁵ A. Bundock¹³⁵ F. Bury¹³⁵
 E. Clement¹³⁵ D. Cussans¹³⁵ H. Flacher¹³⁵ M. Glowacki¹³⁵ J. Goldstein¹³⁵ H. F. Heath¹³⁵ M.-L. Holmberg¹³⁵

- L. Kreczko¹³⁵, S. Paramesvaran¹³⁵, L. Robertshaw¹³⁵, S. Seif El Nasr-Storey¹³⁵, V. J. Smith¹³⁵, N. Stylianou^{135,aaaa},
 K. Walkingshaw Pass¹³⁵, A. H. Ball¹³⁶, K. W. Bell¹³⁶, A. Belyaev^{136,bbbb}, C. Brew¹³⁶, R. M. Brown¹³⁶,
 D. J. A. Cockerill¹³⁶, C. Cooke¹³⁶, K. V. Ellis¹³⁶, K. Harder¹³⁶, S. Harper¹³⁶, J. Linacre¹³⁶, K. Manolopoulos¹³⁶,
 D. M. Newbold¹³⁶, E. Olaiya¹³⁶, D. Petyt¹³⁶, T. Reis¹³⁶, A. R. Sahasransu¹³⁶, G. Salvi¹³⁶, T. Schuh¹³⁶,
 C. H. Shepherd-Themistocleous¹³⁶, I. R. Tomalin¹³⁶, T. Williams¹³⁶, R. Bainbridge¹³⁷, P. Bloch¹³⁷,
 C. E. Brown¹³⁷, O. Buchmuller¹³⁷, V. Cacchio¹³⁷, C. A. Carrillo Montoya¹³⁷, G. S. Chahal^{137,cccc}, D. Colling¹³⁷,
 J. S. Dancu¹³⁷, I. Das¹³⁷, P. Dauncey¹³⁷, G. Davies¹³⁷, J. Davies¹³⁷, M. Della Negra¹³⁷, S. Fayer¹³⁷, G. Fedi¹³⁷,
 G. Hall¹³⁷, M. H. Hassanshahi¹³⁷, A. Howard¹³⁷, G. Iles¹³⁷, M. Knight¹³⁷, J. Langford¹³⁷, J. León Holgado¹³⁷,
 L. Lyons¹³⁷, A.-M. Magnan¹³⁷, S. Malik¹³⁷, M. Mieskolainen¹³⁷, J. Nash^{137,dddd}, M. Pesaresi¹³⁷,
 B. C. Radburn-Smith¹³⁷, A. Richards¹³⁷, A. Rose¹³⁷, K. Savva¹³⁷, C. Seez¹³⁷, R. Shukla¹³⁷, A. Tapper¹³⁷,
 K. Uchida¹³⁷, G. P. Uttley¹³⁷, L. H. Vage¹³⁷, T. Virdee^{137,ff}, M. Vojinovic¹³⁷, N. Wardle¹³⁷, D. Winterbottom¹³⁷,
 K. Coldham¹³⁸, J. E. Cole¹³⁸, A. Khan¹³⁸, P. Kyberd¹³⁸, I. D. Reid¹³⁸, S. Abdullin¹³⁹, A. Brinkerhoff¹³⁹,
 B. Caraway¹³⁹, E. Collins¹³⁹, J. Dittmann¹³⁹, K. Hatakeyama¹³⁹, J. Hiltbrand¹³⁹, B. McMaster¹³⁹, S. Sawant¹³⁹,
 C. Sutantawibul¹³⁹, J. Wilson¹³⁹, R. Bartek¹⁴⁰, A. Dominguez¹⁴⁰, C. Huerta Escamilla¹⁴⁰, A. E. Simsek¹⁴⁰,
 R. Uniyal¹⁴⁰, A. M. Vargas Hernandez¹⁴⁰, B. Bam¹⁴¹, R. Chudasama¹⁴¹, S. I. Cooper¹⁴¹, S. V. Gleyzer¹⁴¹,
 C. U. Perez¹⁴¹, P. Rumerio^{141,eeee}, E. Usai¹⁴¹, R. Yi¹⁴¹, A. Akpinar¹⁴², D. Arcaro¹⁴², C. Cosby¹⁴²,
 Z. Demiragli¹⁴², C. Erice¹⁴², C. Fangmeier¹⁴², C. Fernandez Madrazo¹⁴², E. Fontanesi¹⁴², D. Gastler¹⁴²,
 F. Golf¹⁴², S. Jeon¹⁴², I. Reed¹⁴², J. Rohlf¹⁴², K. Salyer¹⁴², D. Sperka¹⁴², D. Spitzbart¹⁴², I. Suarez¹⁴²,
 A. Tsatsos¹⁴², S. Yuan¹⁴², A. G. Zecchinelli¹⁴², G. Benelli¹⁴³, X. Coubez^{143,aa}, D. Cutts¹⁴³, M. Hadley¹⁴³,
 U. Heintz¹⁴³, J. M. Hogan^{143,ffff}, T. Kwon¹⁴³, G. Landsberg¹⁴³, K. T. Lau¹⁴³, D. Li¹⁴³, J. Luo¹⁴³, S. Mondal¹⁴³,
 M. Narain^{143,a}, N. Pervan¹⁴³, S. Sagir^{143,gggg}, F. Simpson¹⁴³, M. Stamenkovic¹⁴³, N. Venkatasubramanian¹⁴³,
 X. Yan¹⁴³, W. Zhang¹⁴³, S. Abbott¹⁴⁴, J. Bonilla¹⁴⁴, C. Brainerd¹⁴⁴, R. Breedon¹⁴⁴, H. Cai¹⁴⁴,
 M. Calderon De La Barca Sanchez¹⁴⁴, M. Chertok¹⁴⁴, M. Citron¹⁴⁴, J. Conway¹⁴⁴, P. T. Cox¹⁴⁴, R. Erbacher¹⁴⁴,
 F. Jensen¹⁴⁴, O. Kukral¹⁴⁴, G. Mocellin¹⁴⁴, M. Mulhearn¹⁴⁴, D. Pellett¹⁴⁴, W. Wei¹⁴⁴, Y. Yao¹⁴⁴, F. Zhang¹⁴⁴,
 M. Bachtis¹⁴⁵, R. Cousins¹⁴⁵, A. Datta¹⁴⁵, G. Flores Avila¹⁴⁵, J. Hauser¹⁴⁵, M. Ignatenko¹⁴⁵, M. A. Iqbal¹⁴⁵,
 T. Lam¹⁴⁵, E. Manca¹⁴⁵, A. Nunez Del Prado¹⁴⁵, D. Saltzberg¹⁴⁵, V. Valuev¹⁴⁵, R. Clare¹⁴⁶, J. W. Gary¹⁴⁶,
 M. Gordon¹⁴⁶, G. Hanson¹⁴⁶, W. Si¹⁴⁶, S. Wimpenny^{146,a}, J. G. Branson¹⁴⁷, S. Cittolin¹⁴⁷, S. Cooperstein¹⁴⁷,
 D. Diaz¹⁴⁷, J. Duarte¹⁴⁷, L. Giannini¹⁴⁷, J. Guiang¹⁴⁷, R. Kansal¹⁴⁷, V. Krutelyov¹⁴⁷, R. Lee¹⁴⁷, J. Letts¹⁴⁷,
 M. Masciovecchio¹⁴⁷, F. Mokhtar¹⁴⁷, S. Mukherjee¹⁴⁷, M. Pieri¹⁴⁷, M. Quinnan¹⁴⁷, B. V. Sathia Narayanan¹⁴⁷,
 V. Sharma¹⁴⁷, M. Tadel¹⁴⁷, E. Vourliotis¹⁴⁷, F. Würthwein¹⁴⁷, Y. Xiang¹⁴⁷, A. Yagil¹⁴⁷, A. Barzdukas¹⁴⁸,
 L. Brennan¹⁴⁸, C. Campagnari¹⁴⁸, J. Incandela¹⁴⁸, J. Kim¹⁴⁸, A. J. Li¹⁴⁸, P. Masterson¹⁴⁸, H. Mei¹⁴⁸,
 J. Richman¹⁴⁸, U. Sarica¹⁴⁸, R. Schmitz¹⁴⁸, F. Setti¹⁴⁸, J. Sheplock¹⁴⁸, D. Stuart¹⁴⁸, T. Á. Vámi¹⁴⁸, S. Wang¹⁴⁸,
 A. Bornheim¹⁴⁹, O. Cerri¹⁴⁹, A. Latorre¹⁴⁹, J. Mao¹⁴⁹, H. B. Newman¹⁴⁹, G. Reales Gutierrez¹⁴⁹, M. Spiropulu¹⁴⁹,
 J. R. Vlimant¹⁴⁹, C. Wang¹⁴⁹, S. Xie¹⁴⁹, R. Y. Zhu¹⁴⁹, J. Alison¹⁵⁰, S. An¹⁵⁰, M. B. Andrews¹⁵⁰, P. Bryant¹⁵⁰,
 M. Cremonesi¹⁵⁰, V. Dutta¹⁵⁰, T. Ferguson¹⁵⁰, A. Harilal¹⁵⁰, C. Liu¹⁵⁰, T. Mudholkar¹⁵⁰, S. Murthy¹⁵⁰,
 P. Palit¹⁵⁰, M. Paulini¹⁵⁰, A. Roberts¹⁵⁰, A. Sanchez¹⁵⁰, W. Terrill¹⁵⁰, J. P. Cumalat¹⁵¹, W. T. Ford¹⁵¹,
 A. Hart¹⁵¹, A. Hassani¹⁵¹, G. Karathanasis¹⁵¹, N. Manganelli¹⁵¹, A. Perloff¹⁵¹, C. Savard¹⁵¹, N. Schonbeck¹⁵¹,
 K. Stenson¹⁵¹, K. A. Ulmer¹⁵¹, S. R. Wagner¹⁵¹, N. Zipper¹⁵¹, D. Zuolo¹⁵¹, J. Alexander¹⁵²,
 S. Bright-Thonney¹⁵², X. Chen¹⁵², D. J. Cranshaw¹⁵², J. Fan¹⁵², X. Fan¹⁵², S. Hogan¹⁵², P. Kotamnives¹⁵²,
 J. Monroy¹⁵², M. Oshiro¹⁵², J. R. Patterson¹⁵², J. Reichert¹⁵², M. Reid¹⁵², A. Ryd¹⁵², J. Thom¹⁵², P. Wittich¹⁵²,
 R. Zou¹⁵², M. Albrow¹⁵³, M. Alyari¹⁵³, O. Amram¹⁵³, G. Apollinari¹⁵³, A. Apresyan¹⁵³, L. A. T. Bauer¹⁵³,
 D. Berry¹⁵³, J. Berryhill¹⁵³, P. C. Bhat¹⁵³, K. Burkett¹⁵³, J. N. Butler¹⁵³, A. Canepa¹⁵³, G. B. Cerati¹⁵³,
 H. W. K. Cheung¹⁵³, F. Chlebana¹⁵³, G. Cummings¹⁵³, J. Dickinson¹⁵³, I. Dutta¹⁵³, V. D. Elvira¹⁵³, Y. Feng¹⁵³,
 J. Freeman¹⁵³, A. Gandrakota¹⁵³, Z. Gecse¹⁵³, L. Gray¹⁵³, D. Green¹⁵³, A. Grummer¹⁵³, S. Grünendahl¹⁵³,
 D. Guerrero¹⁵³, O. Gutsche¹⁵³, R. M. Harris¹⁵³, R. Heller¹⁵³, T. C. Herwig¹⁵³, J. Hirschauer¹⁵³, L. Horyn¹⁵³,
 B. Jayatilaka¹⁵³, S. Jindariani¹⁵³, M. Johnson¹⁵³, U. Joshi¹⁵³, T. Klijnsma¹⁵³, B. Klima¹⁵³, K. H. M. Kwok¹⁵³,
 S. Lammel¹⁵³, D. Lincoln¹⁵³, R. Lipton¹⁵³, T. Liu¹⁵³, C. Madrid¹⁵³, K. Maeshima¹⁵³, C. Mantilla¹⁵³,
 D. Mason¹⁵³, P. McBride¹⁵³, P. Merkel¹⁵³, S. Mrenna¹⁵³, S. Nahm¹⁵³, J. Ngadiuba¹⁵³, D. Noonan¹⁵³,
 V. Papadimitriou¹⁵³, N. Pastika¹⁵³, K. Pedro¹⁵³, C. Pena^{153,hhhh}, F. Ravera¹⁵³, A. Reinsvold Hall^{153,iiii}

- L. Ristori¹⁵³ E. Sexton-Kennedy¹⁵³ N. Smith¹⁵³ A. Soha¹⁵³ L. Spiegel¹⁵³ S. Stoynev¹⁵³ J. Strait¹⁵³
L. Taylor¹⁵³ S. Tkaczyk¹⁵³ N. V. Tran¹⁵³ L. Uplegger¹⁵³ E. W. Vaandering¹⁵³ A. Whitbeck¹⁵³ I. Zoi¹⁵³
C. Aruta¹⁵⁴ P. Avery¹⁵⁴ D. Bourilkov¹⁵⁴ L. Cadamuro¹⁵⁴ P. Chang¹⁵⁴ V. Cherepanov¹⁵⁴ R. D. Field,¹⁵⁴
E. Koenig¹⁵⁴ M. Kolosova¹⁵⁴ J. Konigsberg¹⁵⁴ A. Korytov¹⁵⁴ K. Matchev¹⁵⁴ N. Menendez¹⁵⁴
G. Mitselmakher¹⁵⁴ K. Mohrman¹⁵⁴ A. Muthirakalayil Madhu¹⁵⁴ N. Rawal¹⁵⁴ D. Rosenzweig¹⁵⁴
S. Rosenzweig¹⁵⁴ J. Wang¹⁵⁴ T. Adams¹⁵⁵ A. Al Kadhim¹⁵⁵ A. Askew¹⁵⁵ S. Bower¹⁵⁵ R. Habibullah¹⁵⁵
V. Hagopian¹⁵⁵ R. Hashmi¹⁵⁵ R. S. Kim¹⁵⁵ S. Kim¹⁵⁵ T. Kolberg¹⁵⁵ G. Martinez,¹⁵⁵ H. Prosper¹⁵⁵
P. R. Prova,¹⁵⁵ M. Wulansatiti¹⁵⁵ R. Yohay¹⁵⁵ J. Zhang,¹⁵⁵ B. Alsufyani,¹⁵⁶ M. M. Baarmand¹⁵⁶ S. Butalla¹⁵⁶
S. Das¹⁵⁶ T. Elkafrawy^{156,ddd} M. Hohlmann¹⁵⁶ R. Kumar Verma¹⁵⁶ M. Rahmani,¹⁵⁶ E. Yanes,¹⁵⁶ M. R. Adams¹⁵⁷
A. Baty¹⁵⁷ C. Bennett,¹⁵⁷ R. Cavanaugh¹⁵⁷ R. Escobar Franco¹⁵⁷ O. Evdokimov¹⁵⁷ C. E. Gerber¹⁵⁷
M. Hawksworth,¹⁵⁷ A. Hingrajiya,¹⁵⁷ D. J. Hofman¹⁵⁷ J. h. Lee¹⁵⁷ D. S. Lemos¹⁵⁷ A. H. Merritt¹⁵⁷ C. Mills¹⁵⁷
S. Nanda¹⁵⁷ G. Oh¹⁵⁷ B. Ozek¹⁵⁷ D. Pilipovic¹⁵⁷ R. Pradhan¹⁵⁷ E. Prifti,¹⁵⁷ T. Roy¹⁵⁷ S. Rudrabhatla¹⁵⁷
M. B. Tonjes¹⁵⁷ N. Varelas¹⁵⁷ M. A. Wadud¹⁵⁷ Z. Ye¹⁵⁷ J. Yoo¹⁵⁷ M. Alhusseini¹⁵⁸ D. Blend,¹⁵⁸
K. Dilsiz^{158,jjjj} L. Emediato¹⁵⁸ G. Karaman¹⁵⁸ O. K. Köseyan¹⁵⁸ J.-P. Merlo,¹⁵⁸ A. Mestvirishvili^{158,kkkk}
J. Nachtman¹⁵⁸ O. Neogi,¹⁵⁸ H. Ogul^{158,III} Y. Onel¹⁵⁸ A. Penzo¹⁵⁸ C. Snyder,¹⁵⁸ E. Tiras^{158,mmmm}
B. Blumenfeld¹⁵⁹ L. Corcodilos¹⁵⁹ J. Davis¹⁵⁹ A. V. Gritsan¹⁵⁹ L. Kang¹⁵⁹ S. Kyriacou¹⁵⁹ P. Maksimovic¹⁵⁹
M. Roguljic¹⁵⁹ J. Roskes¹⁵⁹ S. Sekhar¹⁵⁹ M. Swartz¹⁵⁹ A. Abreu¹⁶⁰ L. F. Alcerro Alcerro¹⁶⁰ J. Anguiano¹⁶⁰
P. Baringer¹⁶⁰ A. Bean¹⁶⁰ Z. Flowers¹⁶⁰ D. Grove¹⁶⁰ J. King¹⁶⁰ G. Krintiras¹⁶⁰ M. Lazarovits¹⁶⁰
C. Le Mahieu¹⁶⁰ J. Marquez¹⁶⁰ N. Minafra¹⁶⁰ M. Murray¹⁶⁰ M. Nickel¹⁶⁰ M. Pitt¹⁶⁰ S. Popescu^{160,nnnn}
C. Rogan¹⁶⁰ C. Royon¹⁶⁰ R. Salvatico¹⁶⁰ S. Sanders¹⁶⁰ C. Smith¹⁶⁰ Q. Wang¹⁶⁰ G. Wilson¹⁶⁰
B. Allmond¹⁶¹ R. Guju Gurunadha¹⁶¹ A. Ivanov¹⁶¹ K. Kaadze¹⁶¹ A. Kalogeropoulos¹⁶¹ Y. Maravin¹⁶¹
J. Natoli¹⁶¹ D. Roy¹⁶¹ G. Sorrentino¹⁶¹ F. Rebassoo¹⁶² D. Wright¹⁶² A. Baden¹⁶³ A. Belloni¹⁶³
Y. M. Chen¹⁶³ S. C. Eno¹⁶³ N. J. Hadley¹⁶³ S. Jabeen¹⁶³ R. G. Kellogg¹⁶³ T. Koeth¹⁶³ Y. Lai¹⁶³
S. Lascio¹⁶³ A. C. Mignerey¹⁶³ S. Nabili¹⁶³ C. Palmer¹⁶³ C. Papageorgakis¹⁶³ M. M. Paranjpe,¹⁶³ L. Wang¹⁶³
J. Bendavid¹⁶⁴ I. A. Cali¹⁶⁴ M. D'Alfonso¹⁶⁴ J. Eysermans¹⁶⁴ C. Freer¹⁶⁴ G. Gomez-Ceballos¹⁶⁴
M. Goncharov,¹⁶⁴ G. Grossi¹⁶⁴ P. Harris,¹⁶⁴ D. Hoang,¹⁶⁴ D. Kovalskyi¹⁶⁴ J. Krupa¹⁶⁴ L. Lavezzi¹⁶⁴ Y.-J. Lee¹⁶⁴
K. Long¹⁶⁴ A. Novak¹⁶⁴ C. Paus¹⁶⁴ D. Rankin¹⁶⁴ C. Roland¹⁶⁴ G. Roland¹⁶⁴ S. Rothman¹⁶⁴
G. S. F. Stephans¹⁶⁴ Z. Wang¹⁶⁴ B. Wyslouch¹⁶⁴ T. J. Yang¹⁶⁴ B. Crossman¹⁶⁵ B. M. Joshi¹⁶⁵ C. Kapsiak¹⁶⁵
M. Krohn¹⁶⁵ D. Mahon¹⁶⁵ J. Mans¹⁶⁵ B. Marzocchi¹⁶⁵ S. Pandey¹⁶⁵ M. Revering¹⁶⁵ R. Rusack¹⁶⁵
R. Saradhy¹⁶⁵ N. Schroeder¹⁶⁵ N. Strobbe¹⁶⁵ L. M. Cremaldi¹⁶⁶ K. Bloom¹⁶⁷ D. R. Claes¹⁶⁷ G. Haza¹⁶⁷
J. Hossain¹⁶⁷ C. Joo¹⁶⁷ I. Kravchenko¹⁶⁷ J. E. Siado¹⁶⁷ W. Tabb¹⁶⁷ A. Vagnerini¹⁶⁷ A. Wightman¹⁶⁷
F. Yan¹⁶⁷ D. Yu¹⁶⁷ H. Bandyopadhyay¹⁶⁸ L. Hay¹⁶⁸ I. Iashvili¹⁶⁸ A. Kharchilava¹⁶⁸ M. Morris¹⁶⁸
D. Nguyen¹⁶⁸ S. Rappoccio¹⁶⁸ H. Rejeb Sfar,¹⁶⁸ A. Williams¹⁶⁸ G. Alverson¹⁶⁹ E. Barberis¹⁶⁹ J. Dervan,¹⁶⁹
Y. Haddad¹⁶⁹ Y. Han¹⁶⁹ A. Krishna¹⁶⁹ J. Li¹⁶⁹ M. Lu¹⁶⁹ G. Madigan¹⁶⁹ R. McCarthy¹⁶⁹ D. M. Morse¹⁶⁹
V. Nguyen¹⁶⁹ T. Orimoto¹⁶⁹ A. Parker¹⁶⁹ L. Skinnari¹⁶⁹ D. Wood¹⁶⁹ J. Bueghly,¹⁷⁰ Z. Chen¹⁷⁰ S. Dittmer¹⁷⁰
K. A. Hahn¹⁷⁰ Y. Liu¹⁷⁰ Y. Miao¹⁷⁰ D. G. Monk¹⁷⁰ M. H. Schmitt¹⁷⁰ A. Taliercio¹⁷⁰ M. Velasco,¹⁷⁰
G. Agarwal¹⁷¹ R. Band¹⁷¹ R. Bucci,¹⁷¹ S. Castells¹⁷¹ A. Das¹⁷¹ R. Goldouzian¹⁷¹ M. Hildreth¹⁷¹
K. W. Ho¹⁷¹ K. Hurtado Anampa¹⁷¹ T. Ivanov¹⁷¹ C. Jessop¹⁷¹ K. Lannon¹⁷¹ J. Lawrence¹⁷¹ N. Loukas¹⁷¹
L. Lutton¹⁷¹ J. Mariano,¹⁷¹ N. Marinelli,¹⁷¹ I. Mcalister,¹⁷¹ T. McCauley¹⁷¹ C. McGrady¹⁷¹ C. Moore¹⁷¹
Y. Musienko^{171,q} H. Nelson¹⁷¹ M. Osherson¹⁷¹ A. Piccinelli¹⁷¹ R. Ruchti¹⁷¹ A. Townsend¹⁷¹ Y. Wan,¹⁷¹
M. Wayne¹⁷¹ H. Yockey,¹⁷¹ M. Zarucki¹⁷¹ L. Zygalas¹⁷¹ A. Basnet¹⁷² B. Bylsma,¹⁷² M. Carrigan¹⁷²
L. S. Durkin¹⁷² C. Hill¹⁷² M. Joyce¹⁷² M. Nunez Ornelas¹⁷² K. Wei,¹⁷² B. L. Winer¹⁷² B. R. Yates¹⁷²
F. M. Addesa¹⁷³ H. Boucharmaoui¹⁷³ P. Das¹⁷³ G. Dezoort¹⁷³ P. Elmer¹⁷³ A. Frankenthal¹⁷³ B. Greenberg¹⁷³
N. Haubrich¹⁷³ G. Kopp¹⁷³ S. Kwan¹⁷³ D. Lange¹⁷³ A. Loeliger¹⁷³ D. Marlow¹⁷³ I. Ojalvo¹⁷³ J. Olsen¹⁷³
A. Shevelev¹⁷³ D. Stickland¹⁷³ C. Tully¹⁷³ S. Malik¹⁷⁴ A. S. Bakshi¹⁷⁵ V. E. Barnes¹⁷⁵ S. Chandra¹⁷⁵
R. Chawla¹⁷⁵ A. Gu¹⁷⁵ L. Gutay,¹⁷⁵ M. Jones¹⁷⁵ A. W. Jung¹⁷⁵ D. Kondratyev¹⁷⁵ A. M. Koshy,¹⁷⁵ M. Liu¹⁷⁵
G. Negro¹⁷⁵ N. Neumeister¹⁷⁵ G. Paspalaki¹⁷⁵ S. Piperov¹⁷⁵ V. Scheurer,¹⁷⁵ J. F. Schulte¹⁷⁵ M. Stojanovic¹⁷⁵
J. Thieman¹⁷⁵ A. K. Virdi¹⁷⁵ F. Wang¹⁷⁵ W. Xie¹⁷⁵ J. Dolen¹⁷⁶ N. Parashar¹⁷⁶ A. Pathak¹⁷⁶ D. Acosta¹⁷⁷
T. Carnahan¹⁷⁷ K. M. Ecklund¹⁷⁷ P. J. Fernández Manteca¹⁷⁷ S. Freed,¹⁷⁷ P. Gardner,¹⁷⁷ F. J. M. Geurts¹⁷⁷

- W. Li¹⁷⁷ O. Miguel Colin¹⁷⁷ B. P. Padley¹⁷⁷ R. Redjimi,¹⁷⁷ J. Rotter¹⁷⁷ E. Yigitbasi¹⁷⁷ Y. Zhang¹⁷⁷
A. Bodek¹⁷⁸ P. de Barbaro¹⁷⁸ R. Demina¹⁷⁸ J. L. Dulemba¹⁷⁸ A. Garcia-Bellido¹⁷⁸ O. Hindrichs¹⁷⁸
A. Khukhunaishvili¹⁷⁸ N. Parmar,¹⁷⁸ P. Parygin^{178,q} E. Popova^{178,q} R. Taus¹⁷⁸ K. Goulianatos¹⁷⁹ B. Chiarito,¹⁸⁰
J. P. Chou¹⁸⁰ S. V. Clark¹⁸⁰ D. Gadkari¹⁸⁰ Y. Gershtein¹⁸⁰ E. Halkiadakis¹⁸⁰ M. Heindl¹⁸⁰ C. Houghton¹⁸⁰
D. Jaroslawski¹⁸⁰ O. Karacheban^{180,dd} I. Laflotte¹⁸⁰ A. Lath¹⁸⁰ R. Montalvo,¹⁸⁰ K. Nash,¹⁸⁰ H. Routray¹⁸⁰
P. Saha¹⁸⁰ S. Salur¹⁸⁰ S. Schnetzer,¹⁸⁰ S. Somalwar¹⁸⁰ R. Stone¹⁸⁰ S. A. Thayil¹⁸⁰ S. Thomas,¹⁸⁰ J. Vora¹⁸⁰
H. Wang¹⁸⁰ H. Acharya,¹⁸¹ D. Ally¹⁸¹ A. G. Delannoy¹⁸¹ S. Fiorendi¹⁸¹ S. Higginbotham¹⁸¹ T. Holmes¹⁸¹
A. R. Kanuganti¹⁸¹ N. Karunarathna¹⁸¹ L. Lee¹⁸¹ E. Nibigira¹⁸¹ S. Spanier¹⁸¹ D. Aebi¹⁸² M. Ahmad¹⁸²
O. Bouhal^{182,0000} R. Eusebi¹⁸² J. Gilmore¹⁸² T. Huang¹⁸² T. Kamon^{182,pppp} H. Kim¹⁸² S. Luo¹⁸²
R. Mueller¹⁸² D. Overton¹⁸² D. Rathjens¹⁸² A. Safonov¹⁸² N. Akchurin¹⁸³ J. Damgov¹⁸³ V. Hegde¹⁸³
A. Hussain¹⁸³ Y. Kazhykarim,¹⁸³ K. Lamichhane¹⁸³ S. W. Lee¹⁸³ A. Mankel¹⁸³ T. Peltola¹⁸³ I. Volobouev¹⁸³
E. Appelt¹⁸⁴ Y. Chen¹⁸⁴ S. Greene,¹⁸⁴ A. Gurrola¹⁸⁴ W. Johns¹⁸⁴ R. Kunawalkam Elayavalli¹⁸⁴ A. Melo¹⁸⁴
F. Romeo¹⁸⁴ P. Sheldon¹⁸⁴ S. Tuo¹⁸⁴ J. Velkovska¹⁸⁴ J. Viinikainen¹⁸⁴ B. Cardwell¹⁸⁵ B. Cox¹⁸⁵
J. Hakala¹⁸⁵ R. Hirosky¹⁸⁵ A. Ledovskoy¹⁸⁵ C. Neu¹⁸⁵ C. E. Perez Lara¹⁸⁵ S. Bhattacharya¹⁸⁶
P. E. Karchin¹⁸⁶ A. Aravind,¹⁸⁷ S. Banerjee¹⁸⁷ K. Black¹⁸⁷ T. Bose¹⁸⁷ S. Dasu¹⁸⁷ I. De Bruyn¹⁸⁷
P. Everaerts¹⁸⁷ C. Galloni,¹⁸⁷ H. He¹⁸⁷ M. Herndon¹⁸⁷ A. Herve¹⁸⁷ C. K. Koraka¹⁸⁷ A. Lanaro,¹⁸⁷
R. Loveless¹⁸⁷ J. Madhusudanan Sreekala¹⁸⁷ A. Mallampalli¹⁸⁷ A. Mohammadi¹⁸⁷ S. Mondal,¹⁸⁷ G. Parida¹⁸⁷
L. Pétré¹⁸⁷ D. Pinna,¹⁸⁷ A. Savin,¹⁸⁷ V. Shang¹⁸⁷ V. Sharma¹⁸⁷ W. H. Smith¹⁸⁷ D. Teague,¹⁸⁷ H. F. Tsoi¹⁸⁷
W. Vetens¹⁸⁷ A. Warden¹⁸⁷ S. Afanasiev¹⁸⁸ V. Andreev¹⁸⁸ Yu. Andreev¹⁸⁸ T. Aushev¹⁸⁸ M. Azarkin¹⁸⁸
I. Azhgirey¹⁸⁸ A. Babaev¹⁸⁸ A. Belyaev¹⁸⁸ V. Blinov,^{188,q} E. Boos¹⁸⁸ V. Borshch¹⁸⁸ D. Budkouski¹⁸⁸
V. Chekhovsky,¹⁸⁸ R. Chistov^{188,q} M. Danilov^{188,q} A. Dermenev¹⁸⁸ T. Dimova^{188,q} D. Druzhkin^{188,qqqq}
M. Dubinin^{188,hhhh} L. Dudko¹⁸⁸ A. Ershov¹⁸⁸ G. Gavrilov¹⁸⁸ V. Gavrilov¹⁸⁸ S. Gninenko¹⁸⁸ V. Golovtcov¹⁸⁸
N. Golubev¹⁸⁸ I. Golutvin¹⁸⁸ I. Gorbunov¹⁸⁸ A. Gribushin¹⁸⁸ K. Ivanov¹⁸⁸ Y. Ivanov¹⁸⁸ V. Kachanov¹⁸⁸
V. Karjavine¹⁸⁸ A. Karneyeu¹⁸⁸ V. Kim¹⁸⁸ M. Kirakosyan,¹⁸⁸ D. Kirpichnikov¹⁸⁸ M. Kirsanov¹⁸⁸
V. Klyukhin¹⁸⁸ O. Kodolova^{188,rrr} D. Konstantinov¹⁸⁸ V. Korenkov¹⁸⁸ V. Korotkikh,¹⁸⁸ A. Kozyrev^{188,q}
N. Krasnikov¹⁸⁸ A. Lanev¹⁸⁸ P. Levchenko^{188,ssss} N. Lychkovskaya¹⁸⁸ V. Makarenko¹⁸⁸ A. Malakhov¹⁸⁸
V. Matveev^{188,q} V. Murzin¹⁸⁸ A. Nikitenko^{188,ttt,rrr} S. Obraztsov¹⁸⁸ V. Oreshkin¹⁸⁸ V. Palichik¹⁸⁸
V. Perelygin¹⁸⁸ S. Petrushanko¹⁸⁸ S. Polikarpov^{188,q} V. Popov¹⁸⁸ O. Radchenko^{188,q} R. Ryutin,¹⁸⁸
M. Savina¹⁸⁸ V. Savrin¹⁸⁸ V. Shalaev¹⁸⁸ S. Shmatov¹⁸⁸ S. Shulha¹⁸⁸ Y. Skovpen^{188,q} S. Slabospitskii¹⁸⁸
V. Smirnov¹⁸⁸ A. Snigirev¹⁸⁸ D. Sosnov¹⁸⁸ V. Sulimov¹⁸⁸ E. Tcherniaev¹⁸⁸ A. Terkulov¹⁸⁸ O. Teryaev¹⁸⁸
I. Tlisova¹⁸⁸ A. Toropin¹⁸⁸ L. Uvarov¹⁸⁸ A. Uzunian¹⁸⁸ A. Vorobyev,^{188,a} N. Voytishin¹⁸⁸ B. S. Yildashev,^{188,uuuu}
A. Zarubin¹⁸⁸ I. Zhizhin¹⁸⁸ and A. Zhokin¹⁸⁸

(CMS Collaboration)

¹*Yerevan Physics Institute, Yerevan, Armenia*²*Institut für Hochenergiephysik, Vienna, Austria*³*Universiteit Antwerpen, Antwerpen, Belgium*⁴*Vrije Universiteit Brussel, Brussel, Belgium*⁵*Université Libre de Bruxelles, Bruxelles, Belgium*⁶*Ghent University, Ghent, Belgium*⁷*Université Catholique de Louvain, Louvain-la-Neuve, Belgium*⁸*Centro Brasileiro de Pesquisas Fisicas, Rio de Janeiro, Brazil*⁹*Universidade do Estado do Rio de Janeiro, Rio de Janeiro, Brazil*¹⁰*Universidade Estadual Paulista, Universidade Federal do ABC, São Paulo, Brazil*¹¹*Institute for Nuclear Research and Nuclear Energy, Bulgarian Academy of Sciences, Sofia, Bulgaria*¹²*University of Sofia, Sofia, Bulgaria*¹³*Instituto De Alta Investigación, Universidad de Tarapacá, Casilla 7 D, Arica, Chile*¹⁴*Beihang University, Beijing, China*¹⁵*Department of Physics, Tsinghua University, Beijing, China*¹⁶*Institute of High Energy Physics, Beijing, China*¹⁷*State Key Laboratory of Nuclear Physics and Technology, Peking University, Beijing, China*

- ¹⁸*Sun Yat-Sen University, Guangzhou, China*
¹⁹*University of Science and Technology of China, Hefei, China*
²⁰*Nanjing Normal University, Nanjing, China*
²¹*Institute of Modern Physics and Key Laboratory of Nuclear Physics and Ion-beam Application (MOE)—Fudan University, Shanghai, China*
²²*Zhejiang University, Hangzhou, Zhejiang, China*
²³*Universidad de Los Andes, Bogota, Colombia*
²⁴*Universidad de Antioquia, Medellin, Colombia*
²⁵*University of Split, Faculty of Electrical Engineering, Mechanical Engineering and Naval Architecture, Split, Croatia*
²⁶*University of Split, Faculty of Science, Split, Croatia*
²⁷*Institute Rudjer Boskovic, Zagreb, Croatia*
²⁸*University of Cyprus, Nicosia, Cyprus*
²⁹*Charles University, Prague, Czech Republic*
³⁰*Escuela Politecnica Nacional, Quito, Ecuador*
³¹*Universidad San Francisco de Quito, Quito, Ecuador*
³²*Academy of Scientific Research and Technology of the Arab Republic of Egypt, Egyptian Network of High Energy Physics, Cairo, Egypt*
³³*Center for High Energy Physics (CHEP-FU), Fayoum University, El-Fayoum, Egypt*
³⁴*National Institute of Chemical Physics and Biophysics, Tallinn, Estonia*
³⁵*Department of Physics, University of Helsinki, Helsinki, Finland*
³⁶*Helsinki Institute of Physics, Helsinki, Finland*
³⁷*Lappeenranta-Lahti University of Technology, Lappeenranta, Finland*
³⁸*IRFU, CEA, Université Paris-Saclay, Gif-sur-Yvette, France*
³⁹*Laboratoire Leprince-Ringuet, CNRS/IN2P3, Ecole Polytechnique, Institut Polytechnique de Paris, Palaiseau, France*
⁴⁰*Université de Strasbourg, CNRS, IPHC UMR 7178, Strasbourg, France*
⁴¹*Institut de Physique des 2 Infinis de Lyon (IP2I), Villeurbanne, France*
⁴²*Georgian Technical University, Tbilisi, Georgia*
⁴³*RWTH Aachen University, I. Physikalisches Institut, Aachen, Germany*
⁴⁴*RWTH Aachen University, III. Physikalisches Institut A, Aachen, Germany*
⁴⁵*RWTH Aachen University, III. Physikalisches Institut B, Aachen, Germany*
⁴⁶*Deutsches Elektronen-Synchrotron, Hamburg, Germany*
⁴⁷*University of Hamburg, Hamburg, Germany*
⁴⁸*Karlsruhe Institut fuer Technologie, Karlsruhe, Germany*
⁴⁹*Institute of Nuclear and Particle Physics (INPP), NCSR Demokritos, Aghia Paraskevi, Greece*
⁵⁰*National and Kapodistrian University of Athens, Athens, Greece*
⁵¹*National Technical University of Athens, Athens, Greece*
⁵²*University of Ioánnina, Ioánnina, Greece*
⁵³*HUN-REN Wigner Research Centre for Physics, Budapest, Hungary*
⁵⁴*MTA-ELTE Lendület CMS Particle and Nuclear Physics Group, Eötvös Loránd University, Budapest, Hungary*
⁵⁵*Faculty of Informatics, University of Debrecen, Debrecen, Hungary*
⁵⁶*Institute of Nuclear Research ATOMKI, Debrecen, Hungary*
⁵⁷*Karoly Robert Campus, MATE Institute of Technology, Gyongyos, Hungary*
⁵⁸*Panjab University, Chandigarh, India*
⁵⁹*University of Delhi, Delhi, India*
⁶⁰*Saha Institute of Nuclear Physics, HBNI, Kolkata, India*
⁶¹*Indian Institute of Technology Madras, Madras, India*
⁶²*Tata Institute of Fundamental Research-A, Mumbai, India*
⁶³*Tata Institute of Fundamental Research-B, Mumbai, India*
⁶⁴*National Institute of Science Education and Research, An OCC of Homi Bhabha National Institute, Bhubaneswar, Odisha, India*
⁶⁵*Indian Institute of Science Education and Research (IISER), Pune, India*
⁶⁶*Isfahan University of Technology, Isfahan, Iran*
⁶⁷*Institute for Research in Fundamental Sciences (IPM), Tehran, Iran*
⁶⁸*University College Dublin, Dublin, Ireland*
^{69a}*INFN Sezione di Bari, Bari, Italy*
^{69b}*Università di Bari, Bari, Italy*
^{69c}*Politecnico di Bari, Bari, Italy*

- ^{70a}INFN Sezione di Bologna, Bologna, Italy
^{70b}Università di Bologna, Bologna, Italy
^{71a}INFN Sezione di Catania, Catania, Italy
^{71b}Università di Catania, Catania, Italy
^{72a}INFN Sezione di Firenze, Firenze, Italy
^{72b}Università di Firenze, Firenze, Italy
⁷³INFN Laboratori Nazionali di Frascati, Frascati, Italy
⁷⁴INFN Sezione di Genova, Università di Genova, Genova, Italy
^{74a}INFN Sezione di Genova, Genova, Italy
^{74b}Università di Genova, Genova, Italy
^{75a}INFN Sezione di Milano-Bicocca, Milano, Italy
^{75b}Università di Milano-Bicocca, Milano, Italy
^{76a}INFN Sezione di Napoli, Napoli, Italy
^{76b}Università di Napoli 'Federico II', Napoli, Italy
^{76c}Università della Basilicata, Potenza, Italy
^{76d}Scuola Superiore Meridionale (SSM), Napoli, Italy
^{77a}INFN Sezione di Padova, Padova, Italy
^{77b}Università di Padova, Padova, Italy
^{77c}Università di Trento, Trento, Italy
^{78a}INFN Sezione di Pavia, Pavia, Italy
^{78b}Università di Pavia, Pavia, Italy
^{79a}INFN Sezione di Perugia, Perugia, Italy
^{79b}Università di Perugia, Perugia, Italy
^{80a}INFN Sezione di Pisa, Pisa, Italy
^{80b}Università di Pisa, Pisa, Italy
^{80c}Scuola Normale Superiore di Pisa, Pisa, Italy
^{80d}Università di Siena, Siena, Italy
^{81a}INFN Sezione di Roma, Roma, Italy
^{81b}Sapienza Università di Roma, Roma, Italy
^{82a}INFN Sezione di Torino, Torino, Italy
^{82b}Università di Torino, Torino, Italy
^{82c}Università del Piemonte Orientale, Novara, Italy
^{83a}INFN Sezione di Trieste, Trieste, Italy
^{83b}Università di Trieste, Trieste, Italy
⁸⁴Kyungpook National University, Daegu, Korea
⁸⁵Department of Mathematics and Physics—GWNU, Gangneung, Korea
⁸⁶Chonnam National University, Institute for Universe and Elementary Particles, Kwangju, Korea
⁸⁷Hanyang University, Seoul, Korea
⁸⁸Korea University, Seoul, Korea
⁸⁹Kyung Hee University, Department of Physics, Seoul, Korea
⁹⁰Sejong University, Seoul, Korea
⁹¹Seoul National University, Seoul, Korea
⁹²University of Seoul, Seoul, Korea
⁹³Yonsei University, Department of Physics, Seoul, Korea
⁹⁴Sungkyunkwan University, Suwon, Korea
⁹⁵College of Engineering and Technology, American University of the Middle East (AUM), Dasman, Kuwait
⁹⁶Riga Technical University, Riga, Latvia
⁹⁷University of Latvia (LU), Riga, Latvia
⁹⁸Vilnius University, Vilnius, Lithuania
⁹⁹National Centre for Particle Physics, Universiti Malaya, Kuala Lumpur, Malaysia
¹⁰⁰Universidad de Sonora (UNISON), Hermosillo, Mexico
¹⁰¹Centro de Investigacion y de Estudios Avanzados del IPN, Mexico City, Mexico
¹⁰²Universidad Iberoamericana, Mexico City, Mexico
¹⁰³Benemerita Universidad Autonoma de Puebla, Puebla, Mexico
¹⁰⁴University of Montenegro, Podgorica, Montenegro
¹⁰⁵University of Canterbury, Christchurch, New Zealand
¹⁰⁶National Centre for Physics, Quaid-I-Azam University, Islamabad, Pakistan
¹⁰⁷AGH University of Krakow, Faculty of Computer Science, Electronics and Telecommunications, Krakow, Poland

- ¹⁰⁸National Centre for Nuclear Research, Swierk, Poland
¹⁰⁹Institute of Experimental Physics, Faculty of Physics, University of Warsaw, Warsaw, Poland
¹¹⁰Warsaw University of Technology, Warsaw, Poland
¹¹¹Laboratório de Instrumentação e Física Experimental de Partículas, Lisboa, Portugal
¹¹²Faculty of Physics, University of Belgrade, Belgrade, Serbia
¹¹³VINCA Institute of Nuclear Sciences, University of Belgrade, Belgrade, Serbia
¹¹⁴Centro de Investigaciones Energéticas Medioambientales y Tecnológicas (CIEMAT), Madrid, Spain
¹¹⁵Universidad Autónoma de Madrid, Madrid, Spain
¹¹⁶Universidad de Oviedo, Instituto Universitario de Ciencias y Tecnologías Espaciales de Asturias (ICTEA), Oviedo, Spain
¹¹⁷Instituto de Física de Cantabria (IFCA), CSIC-Universidad de Cantabria, Santander, Spain
¹¹⁸University of Colombo, Colombo, Sri Lanka
¹¹⁹University of Ruhuna, Department of Physics, Matara, Sri Lanka
¹²⁰CERN, European Organization for Nuclear Research, Geneva, Switzerland
¹²¹Paul Scherrer Institut, Villigen, Switzerland
¹²²ETH Zurich—Institute for Particle Physics and Astrophysics (IPA), Zurich, Switzerland
¹²³Universität Zürich, Zurich, Switzerland
¹²⁴National Central University, Chung-Li, Taiwan
¹²⁵National Taiwan University (NTU), Taipei, Taiwan
¹²⁶High Energy Physics Research Unit, Department of Physics, Faculty of Science, Chulalongkorn University, Bangkok, Thailand
¹²⁷Cukurova University, Physics Department, Science and Art Faculty, Adana, Turkey
¹²⁸Middle East Technical University, Physics Department, Ankara, Turkey
¹²⁹Bogazici University, Istanbul, Turkey
¹³⁰Istanbul Technical University, Istanbul, Turkey
¹³¹Istanbul University, Istanbul, Turkey
¹³²Yildiz Technical University, Istanbul, Turkey
¹³³Institute for Scintillation Materials of National Academy of Science of Ukraine, Kharkiv, Ukraine
¹³⁴National Science Centre, Kharkiv Institute of Physics and Technology, Kharkiv, Ukraine
¹³⁵University of Bristol, Bristol, United Kingdom
¹³⁶Rutherford Appleton Laboratory, Didcot, United Kingdom
¹³⁷Imperial College, London, United Kingdom
¹³⁸Brunel University, Uxbridge, United Kingdom
¹³⁹Baylor University, Waco, Texas, USA
¹⁴⁰Catholic University of America, Washington, DC, USA
¹⁴¹The University of Alabama, Tuscaloosa, Alabama, USA
¹⁴²Boston University, Boston, Massachusetts, USA
¹⁴³Brown University, Providence, Rhode Island, USA
¹⁴⁴University of California, Davis, Davis, California, USA
¹⁴⁵University of California, Los Angeles, California, USA
¹⁴⁶University of California, Riverside, Riverside, California, USA
¹⁴⁷University of California, San Diego, La Jolla, California, USA
¹⁴⁸University of California, Santa Barbara—Department of Physics, Santa Barbara, California, USA
¹⁴⁹California Institute of Technology, Pasadena, California, USA
¹⁵⁰Carnegie Mellon University, Pittsburgh, Pennsylvania, USA
¹⁵¹University of Colorado Boulder, Boulder, Colorado, USA
¹⁵²Cornell University, Ithaca, New York, USA
¹⁵³Fermi National Accelerator Laboratory, Batavia, Illinois, USA
¹⁵⁴University of Florida, Gainesville, Florida, USA
¹⁵⁵Florida State University, Tallahassee, Florida, USA
¹⁵⁶Florida Institute of Technology, Melbourne, Florida, USA
¹⁵⁷University of Illinois Chicago, Chicago, USA, Chicago, USA
¹⁵⁸The University of Iowa, Iowa City, Iowa, USA
¹⁵⁹Johns Hopkins University, Baltimore, Maryland, USA
¹⁶⁰The University of Kansas, Lawrence, Kansas, USA
¹⁶¹Kansas State University, Manhattan, Kansas, USA
¹⁶²Lawrence Livermore National Laboratory, Livermore, California, USA
¹⁶³University of Maryland, College Park, Maryland, USA
¹⁶⁴Massachusetts Institute of Technology, Cambridge, Massachusetts, USA
¹⁶⁵University of Minnesota, Minneapolis, Minnesota, USA

- ¹⁶⁶*University of Mississippi, Oxford, Mississippi, USA*
¹⁶⁷*University of Nebraska-Lincoln, Lincoln, Nebraska, USA*
¹⁶⁸*State University of New York at Buffalo, Buffalo, New York, USA*
¹⁶⁹*Northeastern University, Boston, Massachusetts, USA*
¹⁷⁰*Northwestern University, Evanston, Illinois, USA*
¹⁷¹*University of Notre Dame, Notre Dame, Indiana, USA*
¹⁷²*The Ohio State University, Columbus, Ohio, USA*
¹⁷³*Princeton University, Princeton, New Jersey, USA*
¹⁷⁴*University of Puerto Rico, Mayaguez, Puerto Rico, USA*
¹⁷⁵*Purdue University, West Lafayette, Indiana, USA*
¹⁷⁶*Purdue University Northwest, Hammond, Indiana, USA*
¹⁷⁷*Rice University, Houston, Texas, USA*
¹⁷⁸*University of Rochester, Rochester, New York, USA*
¹⁷⁹*The Rockefeller University, New York, New York, USA*
¹⁸⁰*Rutgers, The State University of New Jersey, Piscataway, New Jersey, USA*
¹⁸¹*University of Tennessee, Knoxville, Tennessee, USA*
¹⁸²*Texas A&M University, College Station, Texas, USA*
¹⁸³*Texas Tech University, Lubbock, Texas, USA*
¹⁸⁴*Vanderbilt University, Nashville, Tennessee, USA*
¹⁸⁵*University of Virginia, Charlottesville, Virginia, USA*
¹⁸⁶*Wayne State University, Detroit, Michigan, USA*
¹⁸⁷*University of Wisconsin—Madison, Madison, Wisconsin, USA*
¹⁸⁸*An institute or international laboratory covered by a cooperation agreement with CERN*

^aDeceased.^bAlso at Yerevan State University, Yerevan, Armenia.^cAlso at TU Wien, Vienna, Austria.^dAlso at Institute of Basic and Applied Sciences, Faculty of Engineering, Arab Academy for Science, Technology and Maritime Transport, Alexandria, Egypt.^eAlso at Ghent University, Ghent, Belgium.^fAlso at Universidade Estadual de Campinas, Campinas, Brazil.^gAlso at Federal University of Rio Grande do Sul, Porto Alegre, Brazil.^hAlso at UFMS, Nova Andradina, Brazil.ⁱAlso at Nanjing Normal University, Nanjing, China.^jAlso at The University of Iowa, Iowa City, Iowa, USA.^kAlso at University of Chinese Academy of Sciences, Beijing, China.^lAlso at China Center of Advanced Science and Technology, Beijing, China.^mAlso at University of Chinese Academy of Sciences, Beijing, China.ⁿAlso at China Spallation Neutron Source, Guangdong, China.^oAlso at Henan Normal University, Xinxiang, China.^pAlso at Université Libre de Bruxelles, Bruxelles, Belgium.^qAlso at Another institute or international laboratory covered by a cooperation agreement with CERN.^rAlso at Suez University, Suez, Egypt.^sAlso at British University in Egypt, Cairo, Egypt.^tAlso at Purdue University, West Lafayette, Indiana, USA.^uAlso at Université de Haute Alsace, Mulhouse, France.^vAlso at Department of Physics, Tsinghua University, Beijing, China.^wAlso at Tbilisi State University, Tbilisi, Georgia.^xAlso at The University of the State of Amazonas, Manaus, Brazil.^yAlso at Erzincan Binali Yildirim University, Erzincan, Turkey.^zAlso at University of Hamburg, Hamburg, Germany.^{aa}Also at RWTH Aachen University, III. Physikalisches Institut A, Aachen, Germany.^{bb}Also at Isfahan University of Technology, Isfahan, Iran.^{cc}Also at Bergische University Wuppertal (BUW), Wuppertal, Germany.^{dd}Also at Brandenburg University of Technology, Cottbus, Germany.^{ee}Also at Forschungszentrum Jülich, Juelich, Germany.^{ff}Also at CERN, European Organization for Nuclear Research, Geneva, Switzerland.^{gg}Also at Institute of Physics, University of Debrecen, Debrecen, Hungary.

- ^{hh} Also at Institute of Nuclear Research ATOMKI, Debrecen, Hungary.
ⁱⁱ Also at Universitatea Babes-Bolyai—Facultatea de Fizica, Cluj-Napoca, Romania.
^{jj} Also at MTA-ELTE Lendület CMS Particle and Nuclear Physics Group, Eötvös Loránd University, Budapest, Hungary.
^{kk} Also at Physics Department, Faculty of Science, Assiut University, Assiut, Egypt.
^{ll} Also at HUN-REN Wigner Research Centre for Physics, Budapest, Hungary.
^{mm} Also at Punjab Agricultural University, Ludhiana, India.
ⁿⁿ Also at University of Visva-Bharati, Santiniketan, India.
^{oo} Also at Indian Institute of Science (IISc), Bangalore, India.
^{pp} Also at Birla Institute of Technology, Mesra, Mesra, India.
^{qq} Also at IIT Bhubaneswar, Bhubaneswar, India.
^{rr} Also at Institute of Physics, Bhubaneswar, India.
^{ss} Also at University of Hyderabad, Hyderabad, India.
^{tt} Also at Deutsches Elektronen-Synchrotron, Hamburg, Germany.
^{uu} Also at Department of Physics, Isfahan University of Technology, Isfahan, Iran.
^{vv} Also at Sharif University of Technology, Tehran, Iran.
^{ww} Also at Department of Physics, University of Science and Technology of Mazandaran, Behshahr, Iran.
^{xx} Also at Helwan University, Cairo, Egypt.
^{yy} Also at Italian National Agency for New Technologies, Energy and Sustainable Economic Development, Bologna, Italy.
^{zz} Also at Centro Siciliano di Fisica Nucleare e di Struttura Della Materia, Catania, Italy.
^{aaa} Also at Università degli Studi Guglielmo Marconi, Roma, Italy.
^{bbb} Also at Scuola Superiore Meridionale, Università di Napoli 'Federico II', Napoli, Italy.
^{ccc} Also at Fermi National Accelerator Laboratory, Batavia, Illinois, USA.
^{ddd} Also at Ain Shams University, Cairo, Egypt.
^{eee} Also at Consiglio Nazionale delle Ricerche—Istituto Officina dei Materiali, Perugia, Italy.
^{fff} Also at Department of Applied Physics, Faculty of Science and Technology, Universiti Kebangsaan Malaysia, Bangi, Malaysia.
^{ggg} Also at Consejo Nacional de Ciencia y Tecnología, Mexico City, Mexico.
^{hhh} Also at Trincomalee Campus, Eastern University, Sri Lanka, Nilaveli, Sri Lanka.
ⁱⁱⁱ Also at Saegis Campus, Nugegoda, Sri Lanka.
^{jjj} Also at National and Kapodistrian University of Athens, Athens, Greece.
^{kkk} Also at Ecole Polytechnique Fédérale Lausanne, Lausanne, Switzerland.
^{lll} Also at Universität Zürich, Zurich, Switzerland.
^{mmm} Also at Stefan Meyer Institute for Subatomic Physics, Vienna, Austria.
ⁿⁿⁿ Also at Laboratoire d'Annecy-le-Vieux de Physique des Particules, IN2P3-CNRS, Annecy-le-Vieux, France.
^{ooo} Also at Near East University, Research Center of Experimental Health Science, Mersin, Turkey.
^{ppp} Also at Konya Technical University, Konya, Turkey.
^{qqq} Also at Izmir Bakircay University, Izmir, Turkey.
^{rrr} Also at Adiyaman University, Adiyaman, Turkey.
^{sss} Also at Bozok Universitetesi Rektörlüğü, Yozgat, Turkey.
^{ttt} Also at Marmara University, Istanbul, Turkey.
^{uuu} Also at Milli Savunma University, Istanbul, Turkey.
^{vvv} Also at Kafkas University, Kars, Turkey.
^{www} Also at stanbul Okan University, Istanbul, Turkey.
^{xxx} Also at Hacettepe University, Ankara, Turkey.
^{yyy} Also at Istanbul University—Cerrahpasa, Faculty of Engineering, Istanbul, Turkey.
^{zzz} Also at Yildiz Technical University, Istanbul, Turkey.
^{aaaa} Also at Vrije Universiteit Brussel, Brussel, Belgium.
^{bbbb} Also at School of Physics and Astronomy, University of Southampton, Southampton, United Kingdom.
^{cccc} Also at IPPP Durham University, Durham, United Kingdom.
^{dddd} Also at Monash University, Faculty of Science, Clayton, Australia.
^{eeee} Also at Università di Torino, Torino, Italy.
^{ffff} Also at Bethel University, St. Paul, Minnesota, USA.
^{gggg} Also at Karamanoğlu Mehmetbey University, Karaman, Turkey.
^{hhhh} Also at California Institute of Technology, Pasadena, California, USA.
ⁱⁱⁱ Also at United States Naval Academy, Annapolis, Maryland, USA.
^{jjj} Also at Bingol University, Bingol, Turkey.
^{kkkk} Also at Georgian Technical University, Tbilisi, Georgia.
^{lll} Also at Sinop University, Sinop, Turkey.
^{mmmm} Also at Erciyes University, Kayseri, Turkey.
ⁿⁿⁿⁿ Also at Horia Hulubei National Institute of Physics and Nuclear Engineering (IFIN-HH), Bucharest, Romania.

^{oooo} Also at Texas A&M University at Qatar, Doha, Qatar.

^{pppp} Also at Kyungpook National University, Daegu, Korea.

^{qqqq} Also at Universiteit Antwerpen, Antwerpen, Belgium.

^{rrr} Also at Yerevan Physics Institute, Yerevan, Armenia.

^{sss} Also at Northeastern University, Boston, Massachusetts, USA.

^{ttt} Also at Imperial College, London, United Kingdom.

^{uuu} Also at Institute of Nuclear Physics of the Uzbekistan Academy of Sciences, Tashkent, Uzbekistan.